The Role of Nitrate in Controlling Iron Release from Sediment during Anoxia in Dimictic, Fresh Water Lakes

by

Eric Michael McQuay

A thesis
presented to the University of Waterloo
in fulfillment of the
thesis requirement for the degree of

Master of Science
in
Earth Sciences

Waterloo, Ontario, Canada, 2018

AUTHOR'S DECLARATION

I hereby declare that I am the sole author of this thesis. This is a true copy of the thesis, including any required final revisions, as accepted by my examiners.

I understand that my thesis may be made electronically available to the public.

Abstract

Recent research suggests the availability of reduced iron (Fe) is key in allowing cyanobacteria to outcompete eukaryotic phytoplankton. Cyanobacteria have a greater need for Fe than their eukaryotic competition and are unable to utilize the oxidized form of Fe(III). This means that Fe can be limiting for cyanobacteria growth as the reduced form, Fe(II), is only readily available under anoxic conditions. When the water just above sediment water interface (SWI) becomes anoxic, the redox potential become low enough for Fe(III) to be reduced to Fe(II). As such, it is important to understand the dynamics of four key redox species affect the redox potential at the SWI: O_2, nitrate (NO_3^-), sulfate (SO_4^{2-}) and Fe.

The overall goal of this thesis is to assess the extent that the presence of NO_3^- at the SWI limits Fe release from lake sediments and the important role this interaction has on cyanobacterial competition. This will be accomplished through four chapters. Chapter 1 provides background information on nutrients, lake stratification, the redox ladder and outlines the current hypothesis for cyanobacterial dominance of phytoplankton blooms. In Chapters 2 the aim was demonstrate that the timing and extent of Fe release from sediment during anoxia can be predicted using five basic redox reactions. This was accomplished by collecting field data at two locations and calculating consumption rates of DO, NO_3^- and SO_4^{2-} as well as the release rate of Fe from the sediment and constructing a parsimonious model. Chapter 3 looks to strengthen the assumptions made in chapter 2. Sediment incubations were conducted to determine whether or not the equations used in the model constructed in chapter 2. Finally Chapter 4 summarizes the findings of this research and proposes future work that would expand on the ideas presented here.

A model was developed that utilizes simple reduction equations of dissolved O_2, NO_3^-, SO_4^{2-} and Fe, rates and rate orders of the reduction of these redox species, determined from previous years of sampling, to predict the timing of Fe release from hypolimnetic sediment in stratified, anoxic lakes. Water samples were collected from the hypolimnion of Sturgeon Bay and Deep Bay bi-weekly during the summer of 2014 and 2015 and were analyzed for concentrations of O_2, NO_3^-, SO_4^{2-} and Fe. It was determined that reduction rates of all key redox species remain consistent between years which means that the only information required to run the model for other years is the initial concentrations of the key redox elements in the late spring/ early summer of the year in question. By using late spring/early summer concentrations of NO_3^-, O_2 and SO_4^{2-} from discrete depths in the water column of the hypolimnion as initial conditions, it was possible to accurately predict the timing of Fe release after stratification to within 10 days of when Fe accumulation was observed in the field in the same year.

Laboratory scale sediment incubations were conducted to observe and ensure that the rate equations for the reduction of the key redox species used in the model are transferable from one system to another even if the specific rates were not. In addition, the potential use of NO_3^- in changing redox conditions at the SWI of an anoxic system was assessed. It was determined that laboratory incubated sediments show 0^{th} order for the reduction of O_2 and Fe and 1^{st} order for the reduction of NO_3^-. It was also found that while initial NO_3^- concentration did delay the timing of Fe release, it had no effect on the rate of Fe release from anoxic sediment once NO_3^- was removed from the system.

The first implication of this research is that the release of Fe from hypolimnetic sediments of stratified lakes, that become anoxic, is able to be modeled by a small number of redox equations allowing for affordable, simple monitoring of lakes. The second implication is that, while the release rate of Fe is constant from year to year under anoxic conditions, the concentration of NO_3^- present at the SWI

can affect the timing of Fe release during the stratification period. As a result, the altering of NO_3^- concentrations of the hypolimnion may be a valid method in reducing the occurrence or duration of cyanobacteria dominated phytoplankton blooms.

Acknowledgments

I would first like to thank both Dr. Jason Venkiteswaran and Dr. Sherry Schiff for giving me the opportunity to work on this project and providing me with edits that helped me develop my ideas into the document presented here.

I would also like to thank Richard Elgood for all the support he provided in the laboratory, both scientifically and psychologically. Without his words of wisdom, and doorway banter, this process would have been far less enjoyable.

I would also like to extend thanks to everyone from the Environmental Geochemistry Laboratory that helped me over the last three years: Jenn Mead for providing moral support during my first poster presentation at a conference. Sarah Sine for constantly encouraging me during the days leading up to the submission deadline when things were looking bleak. Peter Aukes for being a constant source of positive energy around the lab, Janessa Zheng for spending all that time analyzing carbon isotopes that I hope someone will get some use out of. And to all the co-op students that have come and gone thank you for your hours spent taping bottles and tearing blisters trying to stopper bottles.

Finally, I would like to thank all the syringe tip filters, rolls of electrical tape and sharpies that gave their lives in support of proper sample preservation and organization.

Table of Contents

List of Figures

List of Tables

Chapter 1: Introduction

Lakes in south-central Ontario contain over 21% of the world's surface fresh water (Frey and Mutz, 2007) and are used as drinking water sources. Ontario lakes are also crucial to fishing and recreation industries. However, increased nutrient loading from agricultural run-off and urban waste threatens the stability of these sensitive ecosystems. In the late 1960's, phosphorous (P) loading to lakes was at a high, resulting in phytoplankton blooms (a visible layer of phytoplankton biomass) which, once dead, are consumed by heterotrophs leading to a decrease in oxygen (O_2) concentration in the water column. This decrease in O_2 is problematic for ecosystem health, diminishing the habitable zone for many fish and other organisms. It was during this time period that cyanobacteria, a prokaryotic autotrophic bacteria, became a notable nuisance. Blooms that are comprised of over 50% cyanobacteria, by biomass, are especially important because some cyanobacteria have the potential to produce harmful toxins linked to fish and livestock kills as well as, major drinking water bans. In 1970, the Canada Water Act (CWA) was put in place which set limits on nutrient loading in an effort to reduce the occurrence and magnitude of these blooms. While these regulations appeared to limit the occurrence of blooms until 1990, in the last 26 years there has been an increase in reports of potentially toxic cyanobacteria dominated phytoplankton blooms in south-central Ontario. This suggests that our current understanding of what determines if cyanobacteria will dominate phytoplankton blooms is currently incomplete and our ability to predict the probability of these blooms is weak.

1.1 Nutrients

1.1.1 Carbon

Carbon (C) is the basic building block of life used to build long chain hydrocarbons that make up much of organic material. The two major forms of dissolved carbon in lakes are dissolved inorganic carbon (DIC) and dissolved organic carbon (DOC). DIC is carbon in the form of dissolved CO_2, carbonic acid (H_2CO_3), bicarbonate (HCO_3^-), and carbonate (CO_3^{2-}). Dissolved CO_2 is used by autotrophic phytoplankton as an electron acceptor during primary production. DOC is an umbrella term that covers a range of hydrocarbon based molecules. Most DOC is derived from terrestrial run off of decaying terrestrial organic material (Schindler et al., 1997; Mostofa et al., 2013). DOC can be lost via sedimentation (Wetzel, 2001), heterotrophic microbial respiration (Morel and Hering, 1993) and photodegradation (Sinsabaugh and Findlay, 2003). Although C is a key nutrient, most lakes are not C limited and the extent of biomass accumulation is determined by other nutrients, such as nitrogen (N) or phosphorus (P) (Hecky and Kilham, 1988).

1.1.2 Phosphorus

P is most commonly found in minerals (such as apatite: $Ca_5(PO_4)_3OH$) and is taken up by plant roots and incorporated into biomass (Smil, 2000; Ruttenberg, 2003). P enters the aquatic system through the decomposition of terrestrial organic matter in the form of dissolved organic phosphorus (DOP). Soluble P will either be taken up, as orthophosphate, by microbes which eventually die and settle out of the water column, or form complexes with iron hydroxide ($Fe(OH)_3$) particulate that are insoluble and ultimately end up removed from the system as sediment. However, before P is completely sequestered, it can be released from

sediments under anoxic conditions via internal loading. The reduction of insoluble Fe(III)-P complexes release P into the water column where it can be cycled again. This buildup and release of P in sediments causes a legacy effect after periods of high P loading to a lake that develops seasonal anoxia. Increased P in sediments, occurring after high P loading, can be released back into the water column. At the same time, external P sources release P into the surface of a lake. These two fluxes of P cause the overall P concentrations in the lake to be higher until enough P is either, sequestered deep in the sediment, or released through outflow to allow the concentrations to stabilize.

While phytoplankton have a higher N than P requirement, the concentration of P in a lake is typically much lower than that of N (Guildford and Hecky, 2000) and, as such, P is often the limiting nutrient in lakes. This means that, in a system with excess N, the biomass of phytoplankton that a lake can support will be determined by the availability of P.

P loading in the Great Lakes area was the highest in the 1960's - early 1970's (Daloğlu et al., 2012). There have been many efforts to reduce the loading of P into the lakes such as the Great lakes Water Quality Agreement, which was put in place with aims to reduce the amount of P entering the great lakes. For example, part of this agreement was limiting the amount of P in detergents by 8.8% immediately, followed by another 2.2% by the end of the following year (Knud-Hansen, 1994). Since then, P concentrations in lakes have reached and even fallen below target values in all of the Great Lakes (Scavia et al., 2014; Phosphorous Loading Targets, 2015; Dove and Chapra, 2015).

1.1.3 Nitrogen Cycle

Nitrogen Fixation

Nitrogen (important in the construction of DNA and amino acids with are essential to life) is the most abundant element in the atmosphere (>78%). However, many organisms lack the appropriate mechanisms to utilize the gaseous form of nitrogen (N_2). In order for N to enter the biosphere it must first be converted to biologically available forms or fixed. N_2 can be fixed by lightning strikes, specialized microbes or through industrial processes. Lightning strikes transfer enough energy to split the N_2 molecule into two N radicals which then react with oxygen and dissolve into water, converting it to nitrate (NO_3^-). These dissolved nitrates precipitate to the surface of the earth and are taken up by plants. Some organisms, such as cyanobacteria, have the appropriate mechanism to take in N_2 and convert it to ammonia (Equation 1.1). Once N_2 is fixed by microbes it is considered to be particulate organic nitrogen (PON) because it is incorporated into the cell of the organism that fixed it. N can remain in the PON pool if the primary producer is consumed by a consumer. PON can also sink out of the water column should the N-fixing organism die and fall to the sediment.

Equation 1.1 $$N_2 + 3H_2 \rightarrow 2NH_3$$

The final way that N_2 can enter the biosphere is through industrial fixation. The Haber-Bosch process converts atmospheric N_2 to ammonia and this process led to a revolution in the fertilizer industry because, now that NH_3 was readily manufactured, ammonium NO_3^- fertilizers were easier to produce (Farrar et al., 2014). This led to a large increase in urea fertilizers which, when applied to fields, oxidizes to NO_3^- which is highly mobile in water. As a result, one of the largest sources of NO_3^- to lacustrine systems is through runoff from agriculture.

Nitrification

Nitrification is the process in which NH_4^+ is converted to NO_3^- via two oxidation reactions catalyzed by chemoautotrophic bacteria (equation 1.2). NH_4^+ is oxidized by bacteria such as *Nitrosomonas* that specialize in oxidizing ammonium to NO_2^- in order to meet their energy requirements. The second stage in nitrification is the oxidation of NO_2^- to NO_3^- by nitrite oxidizing bacteria such as *Nitrobacter* (Kalff, 2002).

Equation 1.2 $$NH_4^+ + 2O_2 \rightarrow NO_3^- + H_2O + 2H^+$$

Denitrification

Denitrification is the sequential reduction of NO_3^- to N_2 gas. In lakes, denitrification is mediated by facultative anaerobic, heterotrophic bacteria (Knowles, 1982) that use NO_3^- and NO_2^- as terminal electron acceptors in the oxidation of organic matter. The first step is the reduction of NO_3^- to NO_2^- followed by the reduction of NO_2^- to N_2O and ultimately the reduction of N_2O to N_2 gas which can evade out of the lake and return to the atmosphere or be fixed again and re-enter the N cycle of the lake.

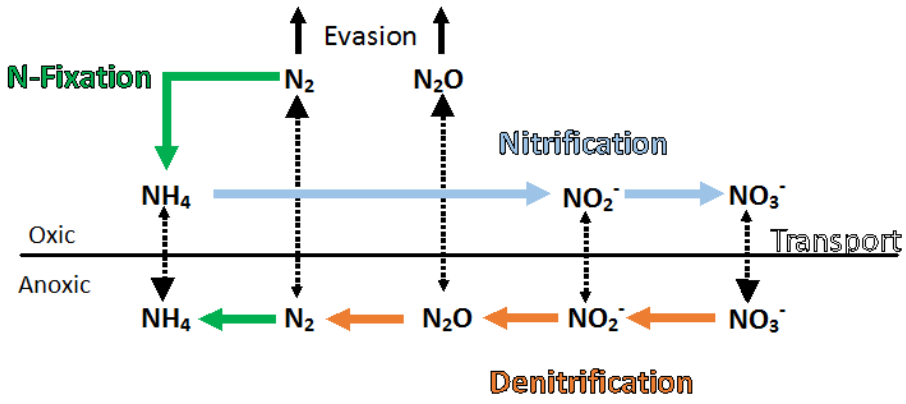

Figure 1.1 Schematic of the N cycle modified from Thamdrup, 2012.

Role of Nitrate in the Cycling of Phosphorus

The N cycle also affects the cycling of other nutrients. Specifically, the presence of NO_3^-, in anaerobic waters, plays a large role in the cycling of Fe and P. When O_2 is available at the SWI, Fe phosphate ($FePO_4$) complexes are insoluble due to the high redox potential present. However, when O_2 is consumed by respiration in the sediment, the redox potential decreases to a point that the Fe-P complexes become soluble in the absence of another electron acceptor. If NO_3^- is present the redox potential is maintained preventing the dissolution of Fe-P complexes limiting the release of phosphorous from sediments.

1.2 Stratification and Redox of Dimictic Lakes

1.2.1 Stratification

Seasonal changes in air temperature affect the mixing dynamics of lakes by causing temperature gradients in the water column. In the summer months, warm air heats the surface water of a lake forming a temperature gradient from the top to the bottom of the lake. This separates the lake into three distinct zones based on density differences: the epilimnion or warm surface layer, the metalimnion where temperature changes by >1 $^oC/m$ and the hypolimnion or cold bottom layer (Figure 1.2). The formation of these layers limits the vertical mixing from the surface of the lake to the bottom to diffusion. If the biological oxygen demand at the SWI is greater than the rate of diffusion of O_2 from the atmosphere, the hypolimnion will become anoxic. Redox conditions at the SWI in the hypolimnion play a major role in lake nutrient cycling. Specifically, the re-release of nutrients from the sediment into the water column during stratification can influence overall nutrient levels (Kalff, 2002).

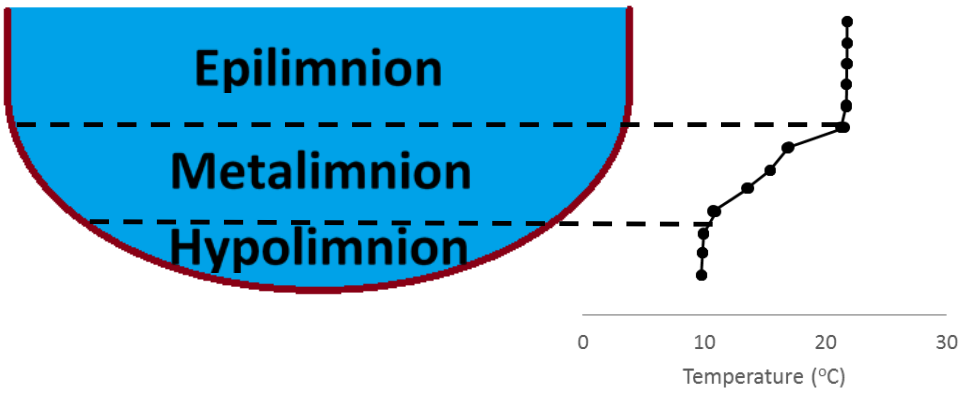

Figure 1.2: Diagram depicting the epi-, meta- and hypolimnion of a temperate lake during stratification. The plot on the right depicts the typical vertical temperature profile observed in well stratified lakes.

1.2.2 Redox

The difference in free energy (G) of the products versus the reactants of a reaction dictate in what direction a chemical reaction will proceed (Engel and Reid, 2005). If the free energy of reactants is greater than the free energy of the products (net negative ΔG) the reaction will proceed toward the products. As ΔG decreases the amount of energy released from a reaction decreases. In the case of microbially mediated redox reactions, the more negative the ΔG is, the more favorable the reaction is and the more energy a microbe will harvest from the reaction. For example, the reduction of O_2 with organic matter has a ΔG° of -2870 kJ/mol whereas the reduction of Fe(III) with organic matter has a ΔG of -1255 kJ/mol meaning that the reduction of O_2 provides the microbe with more energy (Figure 1.3).

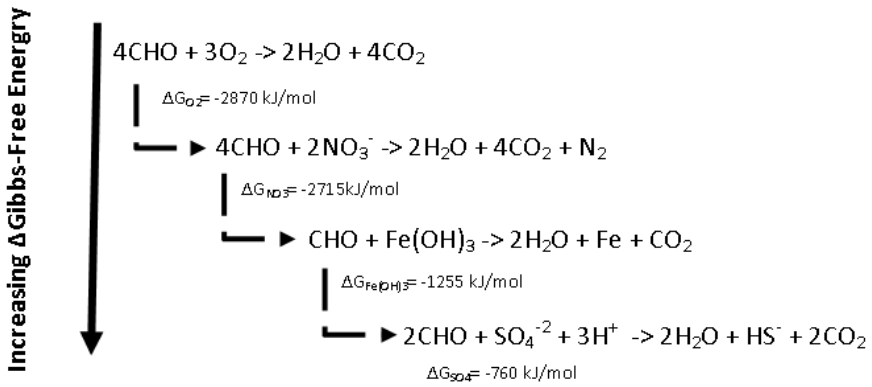

Figure 1.3: The redox ladder of increasing ΔG for the key redox reactions used to develop the simple model. The lower the equation stands on the ladder the less energetically favorable it is. (adapted from Kalff, 2002)

1.2.3 Internal loading

Internal loading is the process in which material from sediment is released back into the water column. In lakes where the hypolimnion becomes anoxic, dissolved Fe concentrations undergo large, rapid increases resulting from internal loading in lakes that experience summer stratification. The release of Fe(II) is dependent on the redox conditions present in a given system. Oxygen and NO_3^- are preferentially used in respiration (as electron acceptors) because they require small amounts of input energy compared to the energies yielded from their respective redox couples. As a result both O_2 and NO_3^- are used as electron acceptors before insoluble Fe(III) is reduced to Fe(II). Hence, at high concentrations, NO_3^- would prevent internal loading of Fe(II) by acting as an intermediate electron acceptor which would delay the timing of Fe(II) release until nearly all the NO_3^- is reduced. SO_4^{2-}, another important electron acceptor, can be reduced to H_2S and reacts with Fe(II) to precipitate insoluble Fe sulfides, reducing the rate at which Fe(II) will accumulate. However, SO_4^{2-} is only reduced under anoxic

conditions when electron acceptors (O_2, NO_3^-, Fe(III)) higher in the redox ladder are depleted. Consequently, SO_4^{2-} reduction does not interfere with Fe(III) reduction.

1.3 Phytoplankton

Eutrophication is an increase nutrient concentration in water bodies caused by anthropogenic activities such as application of fertilizers. These activities can increase the concentration of essential nutrients such as P and N in a lake, thus increasing the lake's capacity to support enhanced biomass (Smith, 1990). During eutrophication, phytoplankton experience rapid growth that results in visible masses that float at or near the surface of affected waterbodies and are referred to here as a blooms. When phytoplankton in a bloom start to decompose, the process consumes O_2 which can impact aquatic life dependent on oxygen for respiration. Also of concern is the dominant species (>50% biomass) in the bloom. Some species of phytoplankton have higher nutrient requirements that others and thus the availability of a specific nutrient may limit the growth of one species while promoting the growth of another (Hecky and Kilham, 1998).

1.3.1 Cyanobacteria

Cyanobacteria area phylum of bacteria (prokaryotic) and are present in most phytoplankton communities around the world. They are also a major concern for water management due to their potential to produce harmful neural toxins. Phytoplankton blooms dominated by cyanobacteria have been responsible for fish kills and the death of livestock that have used impacted lakes as drinking water sources (Havens, 2008). However, cyanobacteria are not only a concern for animals. For instance, a cyanobacteria bloom in 2014 in Lake Erie, near a drinking water intake, caused a drinking water ban that affected hundreds of thousands of inhabitants of Toledo in the summer of 2014 (*E. Fitzsimmons* 7, Aug. 2014). In many lakes

in Ontario, Canada, the number of reports of cyanobacteria dominated blooms have been increasing since the 1990's (Winter, 2011). However, it is still not well understood why cyanobacteria only dominate some phytoplankton blooms.

1.4 Predicting Cyanobacteria Dominance of Phytoplankton Blooms

There are currently two major hypotheses as to what governs cyanobacteria dominance of phytoplankton blooms: N:P in lakes, and the availability of Fe(II).

1.4.1 Hypothesis A: TN:TP Ratios of Lake Water Control Cyanobacteria Dominance of Blooms

It has been proposed that N:P within lake water columns can be used to determine whether N-fixing cyanobacteria will out compete other phytoplankton taxa (Smith, 1983). This hypothesis states that blooms of cyanobacteria will be dominated by N-fixing species if TN:TP in the epilimnion of eutrophic systems is below 29:1. However, this does not mean that TN:TP is useful in predicting if cyanobacteria will dominate phytoplankton blooms in non-eutrophic or eutrophic P-limited, systems.

It has been shown that TP and TN concentrations, independently of each other, predict cyanobacteria abundance (r^2 = 0.34 and 0.42 respectively) better than TN:TP (r^2 = 0.26) suggesting that the risk of cyanobacteria dominance of phytoplankton blooms is greater in systems with higher productivity (Downing et al., 1983).

1.4.2 Hypothesis B: Access to Fe(II) Controls Cyanobacteria Dominance of Blooms.

The second hypothesis states the bioavailability of Fe(II) dictates cyanobacteria dominance (Molot et al., 2014). Cyanobacteria have a higher Fe requirements than other eukaryotic phytoplankton, with N-fixing species of cyanobacteria requiring the most (Wilhelm,

1995, Glass et al., 2009, Molot et al., 2010). This implies that cyanobacteria dominance of phytoplankton blooms may depend more heavily on the availably of reduced Fe and not necessarily on the ratio of TN:TP (Verschoor et al., 2017).

Once in a lake Fe can be taken up by organisms, bind to organic matter and/or sediment out of the water column. Once Fe becomes part of the sediment it remains there and becomes buried and inaccessible to cyanobacteria unless either physical mixing (predominantly in littoral sediment) redistributes it or the redox conditions of the lake change to allow the reduction and subsequent dissolution and diffusion of Fe out of the sediments. The most important of these two redistribution methods with respect to cyanobacteria is the reduction of insoluble Fe(III) to soluble Fe(II) because cyanobacteria are unable to utilize oxidized Fe.

During late spring the epilimnion (surface water) is heated by prolonged contact with warmer air. The warm epilimnetic water is less dense than the cold hypolimnetic water resulting in a density gradient that limits the vertical mixing between the layers. This lack of vertical mixing hinders the transfer of O_2 from the atmosphere to the hypolimnion (Kalff, 2002). This causes the hypolimnion to become depleted in O_2 (anoxic) if the oxygen demand of the sediments is greater than the diffusion rate. Once O_2 is depleted, Fe(III) in the sediment, in the form of $Fe(OH)_3$, will be reduced to Fe(II) which will then dissolve into the water column where cyanobacteria would have greater access. Anoxia may also occur in boundary layers just above littoral sediment. During days with little turbulent mixing a thin boundary layer, typically 1mm in thickness, forms where the rate of physical mixing between sediment and the water column becomes less than the rate of diffusion of dissolved chemical species (Glud et al., 2007). This limits the rate at which oxygen is supplied to the sediment. As a result, anoxia can occur at the SWI even if the water column is oxic. This occurs when the rate of

decomposition at the SWI is greater than the rate of diffusion of oxygen across this boundary layer. The lack of oxygen at the sediment surface would allow for the reduction of Fe(III) which could then be utilized by cyanobacteria living at or near the surface of the sediment.

Altering sediment/water redox may offer a control on Fe release from sediment and thus affect the competition of cyanobacteria and eukaryotes in phytoplankton populations. However, there have been few studies showing the effectiveness of this method (Søndergaard, 2000; Schauser, 2006; Beutel, 2016) and many studies focus on how NO_3^- restricts P release, however Fe release is similarly affected, warranting further study.

1.5 Thesis Objective and Organization

The overall objectives of this thesis are to assess the role of NO_3^- on Fe release from lake sediments because of the important role of NO_3^- and Fe on phytoplankton competition.

The objective of chapter 2 is to construct, and test the ability of, a parsimonious model of linked redox couples to predict the timing and extent of Fe release during the summer stratification of lakes in which the hypolimnion becomes anoxic.

The objective of Chapter 3 is to test the effect of NO_3^- concentration on the release of Fe from anoxic lake sediments.

Chapter 2: Development of an Anoxic Hypolimnion Fe Release Model

2.1 Introduction

Reports of cyanobacteria dominated blooms have been on the rise over the past few decades even in meso- to oligotrophic lakes in central Ontario (Winter et al., 2011). Some cyanobacteria hold the potential to release toxins that impact drinking water quality. These toxins cannot be removed from water via boiling and can completely prevent the use of a particular water body as a drinking water source, as in Toledo during the summer of 2014 (*E. Fitzsimmons*, 7 Aug. 2014; Jetoo et al., 2015). Presently, there are few ways to predict when, where and if a cyanobacteria dominated bloom will occur (Downing et al., 2001). Current explanations as to why cyanobacteria become dominant focus mainly on spring total phosphorous (TP) and total nitrogen (TN) concentrations (Smith, 1983). However, it has recently been proposed that the availability of Fe(II) may have a major role in promoting the dominance of cyanobacteria (Molot, 2014). Cyanobacteria have a large need for Fe(II) because they are unable to transport Fe(III) across their cell membrane. In addition, Fe(II) is used by cyanobacteria in enzymes that reduce NO_3^- and, in some cyanobacteria species, to fix N_2 to NH_4^+ (Sorichetti, 2013). There are a two major ways Fe(II) can become available to cyanobacteria. The first is through the production of siderophores which chelate Fe bound to dissolved organic carbon (DOC) during periods of Fe limitation. Once the chelate is formed, the cyanobacteria can reduce and transport the Fe across the cell membrane where it can be used in metabolic processes. The second, and largest source of Fe(II) in lakes in which the hypolimnion goes anoxic during stratification, is through the reduction of insoluble Fe(III) compounds, such as $Fe(OH)_3$, at the sediment water interface. In the absence of other electron acceptors, mainly O_2 and NO_3^-, facultative anaerobes will utilize $Fe(OH)_3$ compounds as

electron acceptors reducing them and releasing soluble Fe(II) from the sediment to the overlaying water column. Once Fe (III) is reduced to Fe(II) another major factor that controls the release of Fe(II) from sediment is the presence of HS^- from the reduction of SO_4^{2-}, which can react with Fe(II), precipitating it out of solution as insoluble Fe-S compounds. It is thus necessary to understand the processes that dictate and link the fluxes of the key redox species (O_2, NO_3^-, SO_4^{2-} and Fe) during stratification. The interactions between water, sediment, phytoplankton and heterotrophic microbes that govern these processes are numerous and complex. In order to test our understanding of these processes, models are often constructed and then tested with field data.

Many models have been built with this broad goal in mind, and each has its own unique approach to constructing a lake model. One approach is to try to incorporate all the major sources and sinks of specific elements in attempt to create a model of a whole lake that couples atmospheric, water column, sediment and biological processes (Katsev et al., 2006; Couture et al., 2009). This approach has its benefits such as comprehensiveness and the ability to make small alterations to very specific portions of the model. However, the major drawbacks are that these types of models are generally very complex and most importantly, extensive data is required to fit these models to field data. For example, Table 1 shows a list of chemical equations that are used in Katsev et al., 2006. Aside from this list, these models also incorporate other variables affecting physical mixing such as wind speed, temperature and solar radiation. While these types of models are reliable and accurate, the amount of work required to amass the necessary data to fit them to field data can be costly.

Another approach is to create a parsimonious model that assumes that, once a lake becomes thermally stratified, the hypolimnion (Figure 1.2) behaves as a pseudo-closed system.

Vertical mixing rates in the hypolimnion are typically on the scale of m/year which is longer than the stratification period (Kalff, 2002). This implies that the hypolimnion is not well mixed vertically and can be divided into distinct layers that each act as independent systems. This allows the model to ignore the effects of vertical mixing and assume that all changes in concentration occur within each layer. This model also only takes into account the time period after stratification is established.

Table 2.1 List of chemical equations that are considered in the model developed by Katsev et al (2006). This list of 22 equations contrasts in size with the list of 5 equations used in this model (Table 2.2).

Model reactions 'S–X' denotes a species X sorbed to a site S- on solid substrate surface; R' are dissolution rates

No.	Kinetic reactions	Rates
	Primary redox reactions	
1.	$(CH_2O)(NH_3)_y(H_3PO_4)_z + (1+2y)O_2 \rightarrow CO_2 + yNO_3^- + yH^+ + zH_3PO_4 + (1+y)H_2O$	R_{O2}
2.	$(CH_2O)(NH_3)_y(H_3PO_4)_z + 4Fe(OH)_3 + 7CO_2 \rightarrow 4Fe^{2+} + 8HCO_3^- + yNH_3 + zH_3PO_4 + 3H_2O$	$R_{Fe(OH)3}$
3.	$(CH_2O)(NH_3)_y(H_3PO_4)_z + 1/2SO_4^{2-} \rightarrow HCO_3^- + 1/2H_2S + yNH_3 + zH_3PO_4$	R_{SO4}
4.	$(CH_2O)(NH_3)_y(H_3PO_4)_z \rightarrow 1/2CH_4 + 1/2CO_2 + yNH_3 + zH_3PO_4$	R_{CH4}
	Secondary redox reactions	
5.	$4Fe^{2+} + O_2 + 8HCO_3^- + 2H_2O \rightarrow 4Fe(OH)_3 + 8CO_2$	R_{FeOx}
6.	$4S{-}Fe^+ + O_2 + 4HCO_3^- + 6H_2O \rightarrow 4S{-}H^0 + 4Fe(OH)_3 + 4CO_2$	R_{surFe}
7.	$H_2S + 2O_2 + 2HCO_3^- \rightarrow SO_4^{2-} + 2CO_2 + 2H_2O$	R_{SOx}
8.	$FeS + 2O_2 \rightarrow Fe^{2+} + SO_4^{2-}$	R_{FeSOx}
9.	$2Fe(OH)_3 + H_2S + 4CO_2 \rightarrow 2Fe^{2+} + S^0 + 4HCO_3^- + 2H_2O$	R_{SFe3}
10.	$Fe_3(PO_4)_2 + 3H_2S \rightarrow 3FeS + 2H_3PO_4$	R_{Sviv}
11.	$FeCO_3 + H_2S \rightarrow FeS + CO_2 + H_2O$	R_{SFeCO3}
12.	$FeS + H_2S \rightarrow FeS_2 + H_2$	R_{FeSHS}
13.	$2Fe(OH)_3 + FeS + 6CO_2 \rightarrow 3Fe^{2+} + S^0 + 6HCO_3^-$	R_{FeSFe3}
	Mineral precipitation reactions	
14.	$Fe^{2+} + HCO_3^- + HS^- \leftrightarrow FeS + CO_2 + H_2O$	R_{FeS}/R'_{FeS}
15.	$3Fe^{2+} + 2H_3PO_4 + 8H_2O \leftrightarrow Fe_3(PO_4)_2^{\ddagger}8H_2O + 6H^+$	R_{viv}/R'_{viv}
16.	$xFe^{2+} + (1-x)Ca^{2+} + 2HCO_3^- \leftrightarrow Fe_xCa_{(1-x)}CO_3 + CO_2 + H_2O (x=1)$	R_{FeCO3}/R'_{FeCO3}
	Local equilibrium reactions	
	Adsorption	
17.	$H_3PO_4 \leftrightarrow H_3PO_4$ (ads)	
18.	$S{-}H^0 + Fe^{2+} + HCO_3^- \leftrightarrow S{-}Fe^+ + CO_2 + H_2O$	

Acid-base reactions	*Equilibrium constants*
$CO_2(aq) + H_2O \leftrightarrow HCO_3^- + H^+$	$K_{C1}=[H^+][HCO_3^-]/[CO_2]$
$HCO_3^- \leftrightarrow CO_3^{2-} + H^+$	$K_{C2}=[H^+][CO_3^{2-}]/[HCO_3^-]$
$H_2S \leftrightarrow HS^- + H^+$	$K_{HS}=[H^+][HS^-]/[H_2S]$
$H_2O \leftrightarrow H^+ + OH^-$	$K_W=[H^+][OH^-]$

Another assumption made is that all changes in concentrations of key nutrients can be approximated by basic redox reactions near the SWI. The SWI is a region of steep chemical, physical and biological gradients (Santschi, 1990) where electron donors and acceptors are in abundance. It is here that over half of N and C mineralization occurs (Schindler, 1985). Since a majority of the respiration in a lake occurs at the SWI (Pace and Prairie, 2005) it can then be assumed that each reaction occurs in the order they appear on the redox ladder because the more energetically favorable electron acceptors will be utilized first. By assuming changes in electron acceptor concentrations are based on basic redox reactions (Table 2) occuring in the hypolimnion during stratification, it is possible to construct a parsimonious model to predict the timing of Fe release from sediments, in addition to the accumulation of Fe in the hypolimnion after release. It is expected that water column concentrations of O_2, NO_3^- and SO_4^{2-} will decrease over the stratification period due to their use as terminal electron acceptors in the respiration of organic matter. Total dissolved iron (TDFe) will increase because when $Fe(OH)_3$ is reduced in the sediment, it forms Fe(II) which is soluble and will be released into the water column. This model will be useful in determining the best course of action for remediation efforts, of lakes that experience cyanobacteria blooms, that revolve around modifying the redox conditions during stratification (Søndergaard, 2000) or the application of additional redox sensitive materials used to precipitate P from solution (Orihel, 2015).

The overall objectives of this chapter are to:

1. Develop a simple quantitative model that links NO_3^-, SO_4^{2-} and O_2 to Fe release from sediments into the overlying water column of lakes
2. Initialize the model using field data from lakes experience cyanobacteria dominated blooms and those that do not, located in the Georgian Bay area of central Ontario.

3. Assess the model's ability to predict timing of Fe release and rate of Fe accumulation using field data from the same sites during previous years.

2.2 Methods

The model was constructed in order to determine the timing and extent of Fe release (measured as TDFe), as a function of O_2, NO_3^- and SO_4^{2-} in overlaying waters, from sediment during stratification using minimal redox reactions. The key pools are comprised of four important electron acceptors TDFe, NO_3^-, SO_4^{2-} and O_2. STELLA, a visual modeling software which allows construction of models through the visual representation of pools and fluxes, was used because it is an easy to understand program that allows for quick alteration and additions to models. STELLA takes the initial values of each variable and applies their respective fluxes, defined by the model, over the period specified by the time step. In this case the time step was set to 0.1 days to ensure sufficient resolution. This means that for every 0.1 day, STELLA applies the flux equations to the pools and new concentrations are returned. These new values are then used as the concentrations for the next time step. The visual nature of the program allows for simplistic representation (Figure 2.1) of code that is hidden from the user.

2.2.1 Determining Rates

Rates were calculated by plotting concentrations of O_2, NO_3^-, SO_4^{2-} and TDFe, obtained from the field, against time, focusing only on the period of concentration increase or decrease for each species. A linear (0^{th} order) or exponential (first order) trendline was fitted to the data depending which one had a better Pearson correlation coefficient (R^2).

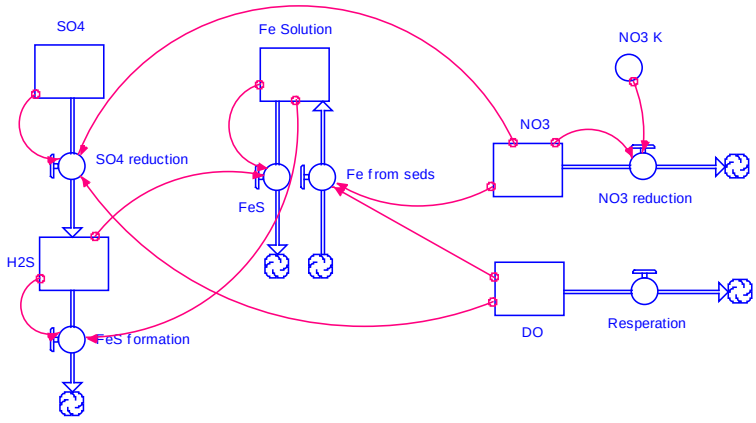

Figure 2.1 The model has 5 stocks; O_2, NO_3^-, Fe Solution, SO_4^{2-} and H_2S that are linked through a series of reactions (Table 2.2). Circles and arrows represent chemical reactions and change in concentration (boxes) redox species. O_2 consumption is modeled as a 0^{th} order reaction and prevents the reduction of Fe and SO_4^{2-} when O_2>0.7 mg/L. Denitrification is modeled by a first-order reaction and controls Fe and SO_4^{2-} reduction when NO_3^- > 0.1 mg/L-N. SO_4^{2-} reduction is also modeled by a first-order reaction and produces H_2S. Once H_2S is available the removal of Fe through FeS formation that is dependent on both the concentration of H_2S and Fe at each time step. Fe release is modeled as a 0^{th} order reaction due to the assumption that sufficient Fe is present in the sediment to maintain a constant rate of Fe release.

Rates used to fit the model to field data were calculated separately for each site and depth studied. For each site, only the rates calculated from a single year's data (Sturgeon Bay & Deep Bay: 2015, L442: 2005, L373: 2006) were used to fit the model to field data and all rates for other years were calculated for comparison. Rates were calculated by taking the slope of the trendline equations for each redox species.

In the case of Fe, it was found that other models express the rate of change concentrations as a second order rate equation (Katsev et al., 2006; Couture et al., 2009). In these models rates are dependent on both the concentration of organic matter (OM) and Fe. However, in this research it is assumed that both OM and Fe are in excess. The models that utilize second order rate equations are modeling the flux of Fe throughout the sediment. As such, the decrease in OM that occurs deeper in the sediment must be taken into account since 75% of OM is consumed in the top 10cm of sediment (Meyers and Ishiwatari, 1993). The

model proposed here only aims to model the interaction at the SWI so OM should remain relatively constant all season. Similarly, Fe concentrations at the SWI are shown to be high enough to sustain continual release during the 100 day stratification season observed during field sampling (Verschoor, unpublished data). With these assumptions it is possible to convert a previously second order rate equation into a 0^{th} order equation. By holding concentrations of OM and Fe constant and combining them with the rate constant (*k*) it is possible to form a pseudo- 0^{th} order rate constant *k'* (Equations 2.1-2.3).

(Equation 2.1) $$Fe_t = [OM]_{t-1}[Fe]_{t-1}e^{kt}$$

(Equation 2.2) $$\frac{dFe_t}{dt}|_i^0 = k[OM]_{i-1}[Fe]_{i-1}$$

(Equation 2.3) $$\frac{dFe_t}{dt} = k'$$

Similarly for SO_4^{2-} and NO_3^-, it is possible to covert second order rate equations into first order rate equations that are only dependent on the concentration of the electron acceptor present in the water column (Equation 2.4-2.6) where k' is an apparent rate constant that is specific to each system.

Equation 2.4 $$A_t = [OM]_{t-1}A_{t-1}e^{-kt}$$

Equation 2.5 $$\frac{dA_t}{dt}|_i^0 = -k[OM]_{i-1}A_{i-1}$$

Equation 2.6 $$\frac{dA_t}{dt}|_i^0 = -k'A_{i-1}$$

In order to model the suppression of both Fe release from sediment and the reduction of SO_4^{2-} in the presence of NO_3^-, a binary function is used to "turn on" Fe release and SO_4^{2-}

reduction at some NO_3^- concentration. Using field observations it was determined that once NO_3^- concentrations drop below 0.2 mg-N/L, there was a large increase in Fe concentration and this value was used as the binary (on-off) switch for both Fe and SO_4^{2-} rates. Other models, such as those described in Katsev, 2006 and Couture, 2009, take into account the effect that the presence of NO_3^- has on redox conditions at the sediment water interface. In the case of Couture, 2009 NO_3^- was not modelled because measures of NO_3^- concentration had poor precision and NO_3^- concentrations were low.

Table 2.2 List of chemical equations used in constructing simplified redox model

	Equations and Highlighted inputs	**Rates**
1.	$CHO + O_2 \rightarrow H_2O + CO_2$	K_{O2}
2.	$4\ CHO + 2\ NO_3^- \rightarrow 2\ H_2O + 4\ CO_2 + N_2$	$k_{NO3}[NO_3^-]$
3.	$2CHO + SO_4^{2-} + 3H^+ \rightarrow 2H_2O + HS^- + 2CO_2$	$k_{SO4}[SO_4^{2-}]$
4.	$CHO + Fe(OH)_3 \rightarrow 2H_2O + Fe + CO_2$	K_{Fe}
5.	$HS^- + Fe^{2+} \rightarrow FeS + H^+$	$k_{FeS}[Fe][HS^-]$

Since only four redox species are considered, the rate for Fe removal from the system was based on the assumption that once O_2 is depleted the main removal of Fe from the system was through the formation of insoluble an Fe-S precipitate. Since only simple redox reactions are considered, it was assumed that all SO_4^{2-} consumed is converted to HS^-. This means that the rate of HS^- formation is equal to the rate of SO_4^{2-} reduction. The last assumption is that once HS^- is present in the system it reacts immediately with available dissolved Fe(II) and that the rate is dictated by the concentration of both Fe and H_2S. This allows Fe to build up before substantial Fe-S precipitation can occur which follows the favorable consumption of electron

acceptors dictated by the redox ladder. The resulting values were entered into their respective boxes and fluxes in the model constructed in STELLA (Figure 2.1).

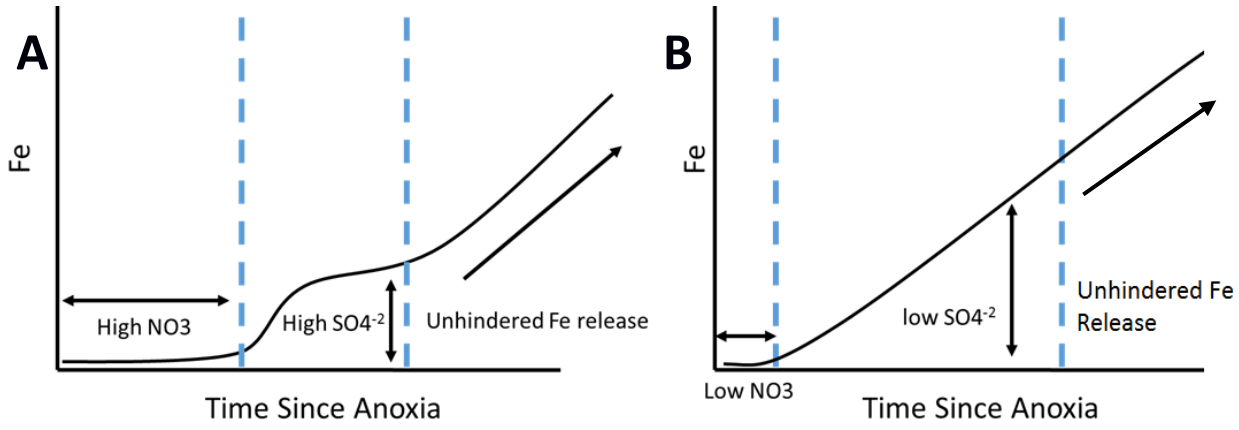

Figure 2.2 A) High initial NO_3^- and SO_4^{2-} concentrations extend the time before Fe release is observed and hinder the release rate of Fe respectively. B) If concentrations of NO_3^- and SO_4^{2-} are sufficiently low Fe release will be observed close to the onset of anoxia and release rates will be constant.

Table 2.3. Assumptions made in the construction of the anoxic hypolimnion Fe release model. These assumptions are examined in the discussion

- All rates calculated from field data are net rates and include biological, physical and chemical factors since only net changes in total dissolved concentrations, were measured
- Microbially labile organic matter is in excess and thus sufficient to keep changes in first order decomposition rates dependent on only the concentration of the electron acceptor
- Before stratification Δ[Fe]=0
- All Fe concentrations are Total Dissolved Fe (TDFe) concentrations
- SO_4^{2-} reduction to H_2S and Fe loading do not occur until NO_3^- is depleted below 0.2 mg-N/L. Determined from field data
- Fe release is instantaneous and follows 0 order rate kinetics once NO_3^- is depleted
- All SO_4^{2-} removed from system is turned into H_2S
- FeS formation occurs as soon as H2S is available. $R_{fe} = -k_{so4}[H_2S][Fe]$.

- When H_2S is low, there is little to no Fe removal, during anoxia, in acidic-neutral lakes
- All H_2S and Fe removed occurs through FeS precipitation
- Hypolimnion layers act as closed systems and experience no vertical mixing since the vertical transfer of redox species is limited to diffusion which is orders of magnitude slower than physical mixing rates. (Kalff, 2002)
- Fe release and O_2 consumption rates are linear with time
- NO_3^- and SO_4^{2-} consumption rates are first order which means that the rate of consumption at a given time is dependent on the concentration of the redox species at that time.

2.2.2 Sample sites

Sturgeon Bay is located near the East shore of Georgian Bay (45.61, -80.43) approximately 45 km north of Parry Sound (Figure 2.3). This area has a geology dominated by grey, leucocratic migmatite with intrusions of pink, leucocratic gneiss (Culshaw et al., 2004). Sturgeon Bay has a surface area of 5.56 km^2 and a maximum depth of 13 m. Sturgeon Bay is heavily developed with several marinas, tourist resorts and a provincial park, Sturgeon Bay Provincial Park (Schiefer, 2003). Surface sediment is fine grained, unconsolidated and easily disturbed. Sturgeon Bay has been known to have algal blooms, that occur almost every year, dominated by cyanobacteria (GBBR, 2013).

Deep Bay is located 15 km northwest of Parry Sound (45.39, -80.22) and has a maximum depth of 18 m and a surface area of 2.85 km^2 (Figure 2.3). The geology of this site is predominately mafic gneiss and migmatite, with surficial deposits of till, sand and silty clay (Miller, 1987). The majority of the shore line of Deep Bay is forested with hard woods such as balsam poplar, black ash and the softwood, black spruce. Further upland where it is drier, forests are comprised of sugar maple, red pine and white birch trees. The shore line is

characterized by steep bedrock outcrops with thin soils that promote the growth of shorter vegetation such as juniper bushes, blueberry and sweet fern (Deep Bay Association, 2012). The sampling location is located in the south western limb near the outlet to Collin's Bay. The deep basin has a slope of 24 cm/m on the south side and a slope of 4cm/m on the north side. Deep Bay has a similar amount of development as the north basin of Sturgeon Bay and, according to land owners, experiences very few observed algae blooms.

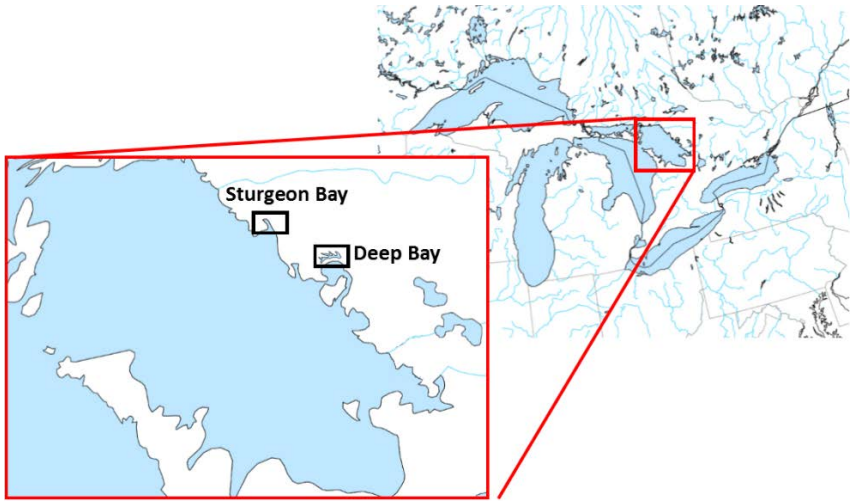

Figure 2.3 Map of Southern Ontario and Georgian Bay showing the location of sampling sites Sturgeon Bay and Deep Bay.

Experimental Lakes Area (ELA)

Lake 442 (49.77, -93.81) and Lake 373 (49.74, -93.79) are both oligotrophic lakes located in ELA in northern Ontario. Historical data from both lakes was used to examine the applicability of the model developed here to predict the timing of Fe release. The geology of ELA is dominated by Precambrian Shield granites and the predominant vegetation is soft wood trees such as Jack pine, white birch and black spruce (Brunskill and Schindler, 1971). These lakes have no development other than a gravel road that few vehicles use since access to these roads is granted for research purposes only.

2.2.3 Depth Profiles for Georgian Bay Sites

Temperature and physiochemical (DO, pH, Oxygen Reduction Potential) profiles were acquired using an YSI sonde. Triplicate measurements were recorded for every meter of depth from the surface down to the sediment surface. Temperature readings were used to construct a temperature profile and determine the thicknesses of the epi-, meta- and hypolimnion where the metalimnion is defined as the area where temperature decreases are greater than 1 ^{o}C/m and the epilimnion and hypolimnion are defined as the areas above and below the metalimnion respectively.

2.2.4 Water Chemistry

In 2014, all water samples were collected using a Wildco® Alpha^{TM} Horizontal Water sampler. Epilimnion samples were collected every meter and integrated evenly by volume in a 4 L acid washed bottle. Subsampling was conducted from this bottle. Metalimnion samples were collected using a similar method. Samples for TP and TN were collected straight from this bottle into acid washed 50 mL centrifuge tubes. Anion samples were filtered in the field through 0.45 µm filters and collected in 25 mL Nalgene® bottles. NH_4^+ and NO_3^- samples were similarly filtered and collected in 25 mL Nalgene® bottles Dissolved Fe and P samples were filtered through 0.2 µm filters into 15 mL and 50 mL bottles, respectively. Fe samples were acidified using concentrated (85 %) trace metal nitric acid. Hypolimnion samples were collected every 2 m to the SWI. These samples were collected using the same horizontal sampler as for the epi- and metalimnion, however, once brought onboard, a rubber tube was connected to an outlet and samples were filtered straight from the sampler to prevent oxidation of anoxic waters. TDP and TP samples were analyzed at the MOECC'S Dorset Environmental Science Centre, Fe samples were analyzed with ICP-MS at the Trent Water Quality Center and

Anion samples were analyzed on a Dionex IC-2000 at the University of Waterloo Environmental Geochemistry lab for NO_3^-, SO_4^{2-}, F^-, Cl^- and Br^-, with a detection limit of 0.05 mg/L and error of ±0.02 mg/L. All other samples were analyzed at the Biogeochemical Analytical Service Laboratory (BASL) at the University of Alberta.

In 2015, additional ICP samples, to be analyzed for Fe, Mn and S, were collected and acidified with concentrated HNO_3. These samples were analyzed at the Centre for Cold Regions and Water Science at Wilfrid Laurier University. Error on TDFe concentrations measurements was ±0.08mg/L which means that the functional detection limit for TDFe samples was 0.16 mg/L.

2.2.5 Normalizing Rates for Sediment Surfacearea

Rates were calculated for the bottom two depths sampled at each site and each rate corresponds to a 2 m thick hypolimnetic interval since samples were collected every 2 m in the hypolimnion. Rates were calculated using field data and fitting trend lines to the period where the greatest decrease (for O_2, NO_3^- and SO_4^{2-}) or increase (Fe) was observed.

Once rates were determined they were converted from mg/L/day to mg/m^2/day by multiplying by volume and dividing by sediment surface area to normalize for lake bottom surface area in order to compare how rates change with depth. The rates were normalized based on the assumption that the surface area of the bottom of a lake could beapproximated by assuming a frustum (truncated cone) shape and excluding the top and bottom surface areas for depths above the bottom of the lake where r is the radius of the deeper layer, R is the radius of the shallower layer (where R > r) and h is the distance between the two depths all in meters (Equation 2.7). This also required the assumption that the contours of each depth could be

converted to an aerial surface area and, using the equation for the surface area of a circle, a radius could be determined.

Equation 2.7 $$Lateral\ Surface\ area = \pi(R + r)\sqrt{(R - r)^2 + h^2}$$

For the bottom depth a frustum was again used but only the top surface area was subtracted and the bottom of the lake was assumed flat (Equation 2.8).

Equation 2.8 $$Bottom\ Surface\ area = \pi(R + r)\sqrt{(R - r)^2 + h^2} + \pi r^2$$

Volume of the section of lake modeled was calculated similarly and converted from m^3 to L by multiplying by 1000. (Equation 2.8)

Equation 2.9 $$Volume = \frac{\pi}{3}h(R^2 + r^2 + R * r) * 1000L/m^3$$

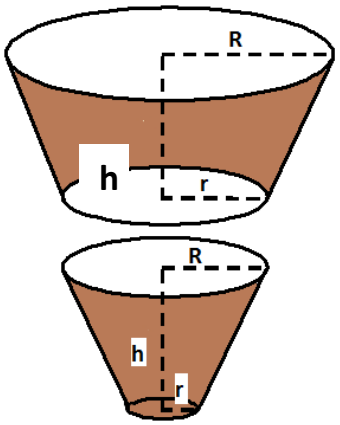

Figure 2.4 Representation of how sediment surface area was calculated assuming a frustum shape for lakes. The shaded areas show those that were included in the calculations for top: any depth above the bottom, and bottom: the bottom depth measured. Vertical and horizontal scales are exaggerated for clarity.

2.2.6 Testing the model

Once rates of O_2, NO_3^- and SO_4^{2-} consumption and Fe release were determined, they were used to initiate the model for each lake and depth independently of each other. These rates were then used to assess the model's ability to predict the timing of Fe release from the sediment, in other years where data was available.

Once the model was run, statistics were calculated to assess how well the model output fit the field data. Root Mean Square Error (RMSE) measures the difference between field data and model result with lower RMSE meaning less discrepancy between the two (equation 2.4). By comparing RMSE calculated from each depth and year it can be determined where the model best estimates Fe release.

Equation 2.4

$$RMSE = \sqrt{\frac{\sum_{i=1}^{n}(X_{obs,i} - X_{model,i})^2}{n}}$$

Another statistical method used to determine how well the model predicts Fe concentrations during stratification is the Nash-Sutcliffe coefficient (E) which is a measure of whether or not the model's predictions are more or less accurate than using an average of observed values. The range of E is $-\infty$ to 1. The closer E is to 1, the closer the predicted concentration of Fe is (X_{model}) to the observed concentration at a given time ($X_{obs,i}$). The further away from 1 E becomes the closer the observed concentrations become to the average of all observed values rather than the predicted values (Equation 2.5).

Equation 2.5

$$E = 1 - \frac{\sum_{i=1}^{n}(X_{obs,i} - X_{model})^2}{\sum_{i=1}^{n}(X_{obs,i} - \overline{X_{obs}})^2}$$

2.3 Results

2.3.1 Temporal Trends of the Hypolimnion

Sturgeon Bay

O_2 , NO_3^- and SO_4^{2-} decreased and Fe increased over the stratification period at both 10 and 12 m depths measured in the hypolimnion in 2015. At the start of the stratification period O_2 concentrations at 10 m and 12 m were 3.2 mg/L and 2.0 mg/L respectively. The O_2 concentration dropped below 0.1 mg/L after 23 days at both depths, with the rate of O_2 consumption being higher at 10 m than at 12 m. After the initial decrease, the O_2 concentration remained low at both depths and did not increase until the end of the stratification period in late September. NO_3^- concentrations were higher (0.2 mg-N/L) at 12 m than at 10 m (0.1 mg-N/L) at the start of the season however, by the end of the stratification period NO_3^- were higher (1 mg-N/L) at 10m than at 12m (0.15 mg-N/L). At both depths NO_3^- concentrations decreased below 0.05 mg-N/L after 42 days, then increased to 0.1 mg-N/L and remained relatively stable for the rest of the stratification period. SO_4^{2-} concentrations in both 10 m and 12 m started at 3.5 mg/L and remained constant for 23 days at which time the concentrations began to decrease. At 10 m depth SO_4^{2-} concentrations decreased by only 0.5 mg/L over the duration of stratification then increased to 4.6 mg/L after turn over in late September. At 12 m depth SO_4^{2-} concentrations decreased to 0.5 mg/L during stratification. Fe concentrations at the start of the season for 10 m and 12 m were 0.20 mg/L and 0.28 mg/L respectively. Fe release began 14 days after first sampling at 12 m and 23 days after sampling at 10 m. Fe concentrations increased to 7.70 mg/L at 12 m by the end of the stratification period. At 10 m Fe concentrations only reached 3.14 mg/L by early September then decreased rapidly to 0.79 mg/L by the end of September when overturn began (Figure 2.5).

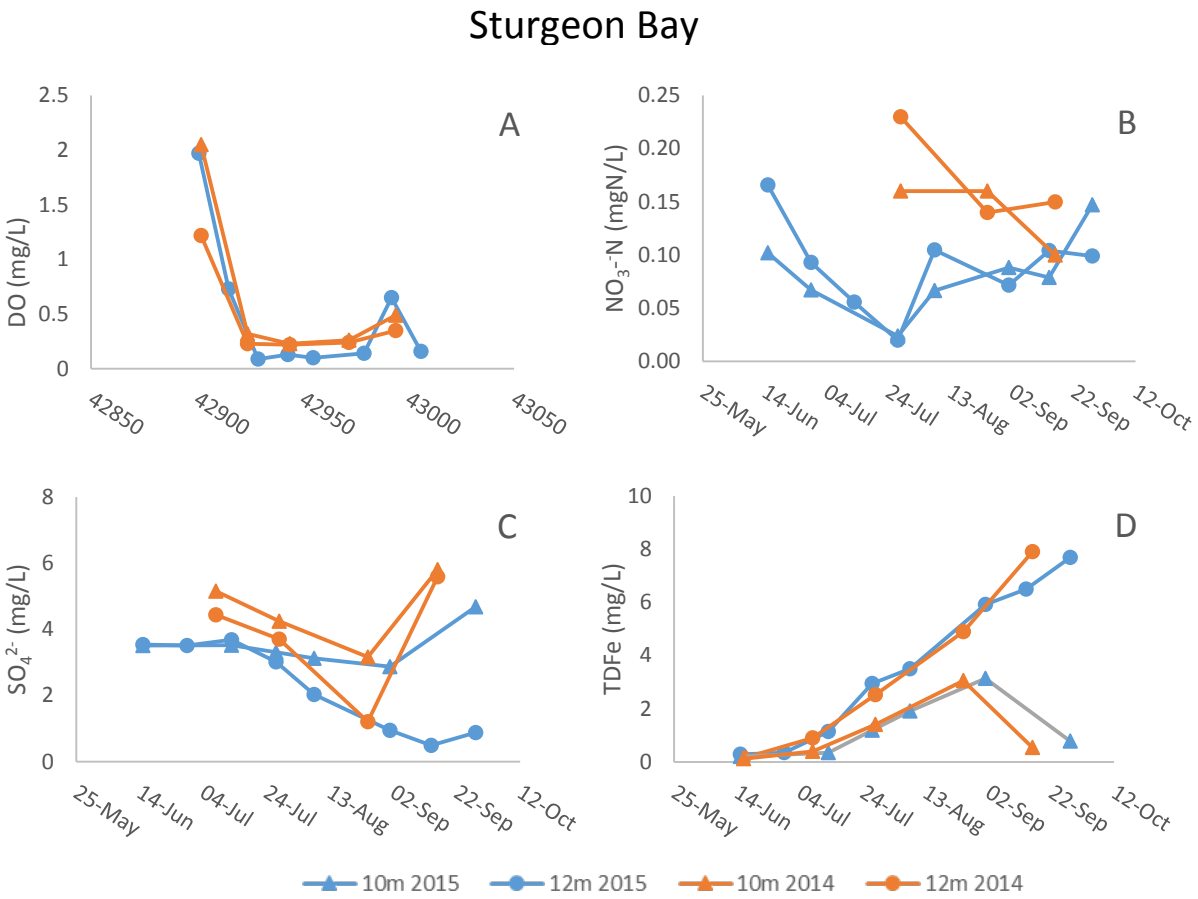

Figure 2.5 Sturgeon Bay 10 m (triangles) and 12 m (circles) hypolimnetic concentration trends of A: O_2, B: NO_3^-, C: SO_4^{2-} and D: TDFe during stratification in 2014 (orange) and 2015 (blue).

Similar trends were observed in 2014 with a few exceptions. First, O_2 concentrations at both 10 m and 12 m (2.05 mg/L and 1.22 mg/L) were lower at the start of the summer compared to 2015. Secondly, NO_3^- concentrations were also higher (0.16 mg-N/L at 10 m and 0.23 mg-N/L at 12 m) in 2014 and the decrease in NO_3^- was not as substantial, only ever reaching 0.1 mg-N/L (Figure 2.5). Finally, decreases in SO_4^{2-} was largely isolated to a single day at the end of August with higher concentrations in both directions and, at 12 m, SO_4^{2-} concentrations increased by a factor of 5 by the final date in mid-September when the hypolimnion disappeared. Fe concentrations follow nearly identical trends in 2014 and 2015

with the exception that, in 2014, higher concentrations were observed by the end of the stratification than in 2015 (7.9 mg/L versus 6.5 mg/L).

Deep Bay

Generally concentrations of O_2, NO_3^- and SO_4^{2-} decreased and Fe increasesed over the course of stratification in Deep Bay in 2015. O_2 concentrations at 16 and 18 m were 4.02 mg/L and 3.52 mg/L at the start of the stratification period and decrease similarly for 42 days until depleted at both depths at which point concentrations at both depths increased to 0.17 mg/L and remained consistent for the remainder of stratification. NO_3^- concentrations increased for the first 23 days of the season. After 23 days NO_3^- begins to decrease to 0.12 mg-N/L at 16m and 0.08 at 18 m and remain steady until turn over in late September. Initial SO_4^{2-} concentrations were 4.50 mg/L and 4.39 mg/L for 16 m and 18 m, respectively. SO_4^{2-} concentrations remained constant for 23 days after which only minor decreases occurred in both depths until the end of stratification. Fe release mirrors the consumption of NO_3^-. In the first 23 days, minimal Fe release was observed. Once NO_3^- concentrations started to decrease, Fe accumulation in the water column increased rapidly reaching 5.92 mg/L after 56 days and remained stable for 14 days before decreasing when NO_3^- began to increase during turn over (Figure 2.6).

Similar trends for SO_4^{2-} and O_2 are seen in 2014 field data while trends for NO_3^- and Fe appeared different. In 2014, NO_3^- concentrations at 16 m decreased from 0.19 mg-N/L to 0.09 mg-N/L and remained constant over the whole stratification period. At 18 m NO_3^- concentrations increased from 0.15 mg-N/L to 0.41 mg-N/L over the stratification period then decreased rapidly to 0.09 mg-N/L in late September. Fe concentrations, in 2014, remained

below 1 mg/L for a majority of the season and the only increase was observed on the final day of sampling in late September (Figure 2.5).

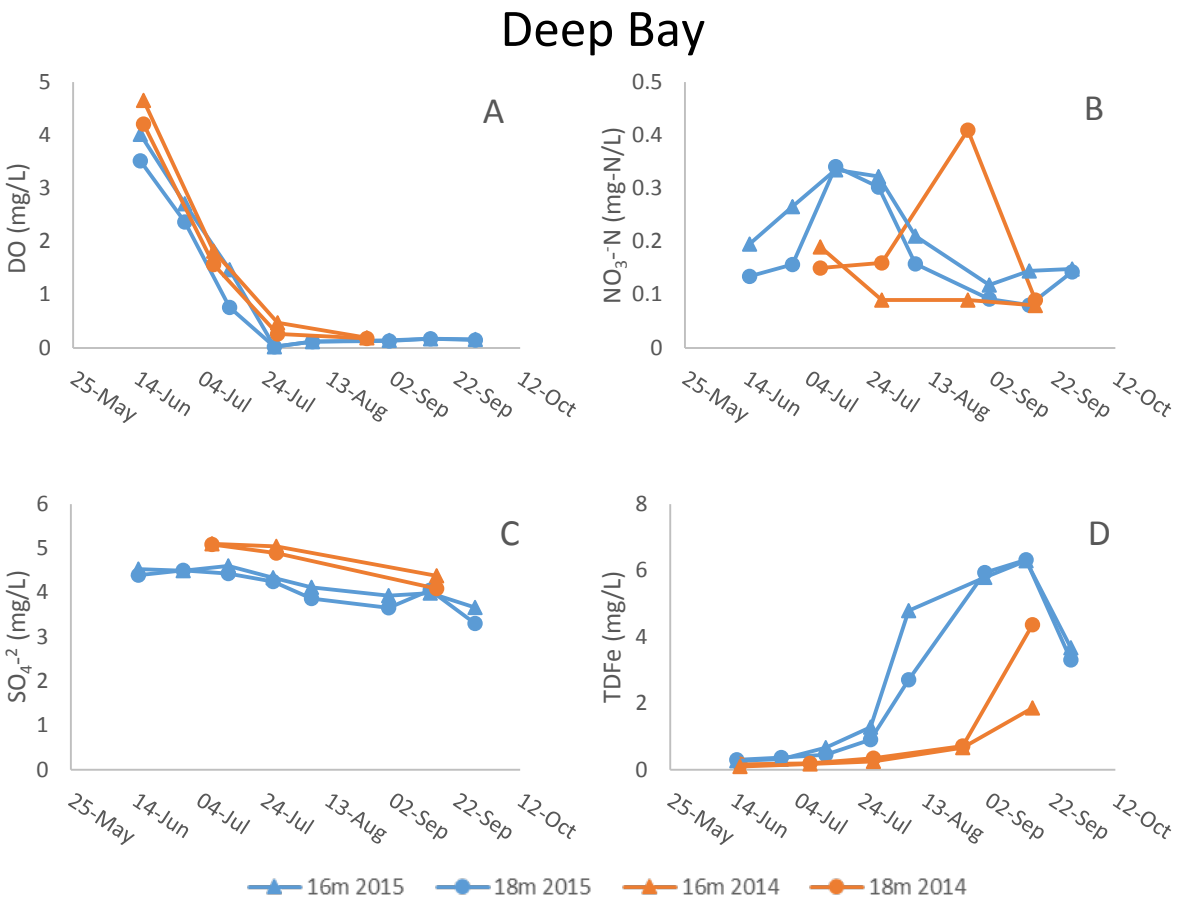

Figure 2.6 Deep Bay 16 m (triangles) and 18 m (circles) hypolimnetic concentration trends of (A) O_2, (B) NO_3^-, (C) SO_4^{2-} and (D) TDFe during stratification in 2014 (orange) and 2015 (blue).

Initial O_2 concentrations were higher (4 mg/L versus 2 mg/L) in the bottom 4 meters of Deep Bay than Sturgeon Bay. O_2 concentrations in Deep Bay only drop below 1 mg/L 23 days after initial sampling whereas, in Sturgeon Bay, O_2 drops below 1 mg/L after 14 days. Initial NO_3^- concentrations at 16 and 18 m in Deep Bay are similar to those seen in 10 and 12 m in Sturgeon Bay but, in Deep Bay NO_3^- increases for a period before decreasing, unlike in Sturgeon Bay where NO_3^- decreases from initial concentrations. SO_4^{2-} decreases by 3 mg/L

over the summer in Sturgeon Bay where as in Deep Bay, even though initial SO_4^{2-} concentrations are similar to Sturgeon Bay, SO_4^{2-} concentrations only decrease by 1 mg/L. Fe concentrations increase linearly in Sturgeon Bay and from the time period from early June to late September no decrease in Fe is observed at 12 m. In Deep Bay Fe accumulation appears to be affected by the presence of NO_3^- later in the season resulting in a decrease in Fe concentration during the month of September when the stratification ends.

ELA Lakes

Lake 442 samples were taken at 13 and 17 m in 2005 and 2006. O_2 concentrations in L442 in 2006 start at 1.91 mg/L and 0.43 mg/L at 13 m and 17 m. O_2 concentrations at 17 m decreased past the detection limit in the first 53 days after first sampling and did not increase (Figure 2.6). At 13 m O_2 remained constant at 1.85 mg/L for the first 23 days after initial sampling and then decreased to 0.2 mg/L by 53 days after sampling. In 2005, initial O_2 concentrations were higher than in 2006 at 5 and 2.67 mg/L at 13 and 17 m. O_2 at both depths in 2005 decreased slowly over the course of the whole stratification season reaching a minimum of 0.2 mg/L after 90 days for both depths. Initial NO_3^- concentrations at all depths and all years are similar ranging from 0.16 to 0.12 mg-N/L. In 2006 NO_3^- concentrations decrease from the initial sampling date decreased below the detection limit by 23 and 53 days after sampling, at both 13 m and 17 m. In 2005 NO_3^- concentrations do not change until 36 days after sampling, at 13 m, at which point the NO_3^- concentration increases to 0.26 mg-N/L then decreases to past the detection limit by the end of stratification. At 17 m NO_3^- concentration decreases steadily over the first 65 days, after which it decreases rapidly passing below the detection limit after 90 days. All SO_4^{2-} concentrations were similar at the first sampling day during the stratification period (1.82-1.67 mg/L) and all decreased at roughly the

same rate. End of summer SO_4^{2-} concentrations also reach similar values (1.57-1.2 mg/L) with little deviation with the exception of 17 m. At 17 m, in 2006, SO_4^{2-} decrease from 0.44 mg/L to 1.23 mg/L in the first 23 days then the rate decreases and the final concentration reached 0.83 mg/L. All Fe concentrations start at 0 mg/L and increase over the summer. In general Fe release does not occur at each depth, in both years, until NO_3^- concentrations drop 0.15 mg-N/L.

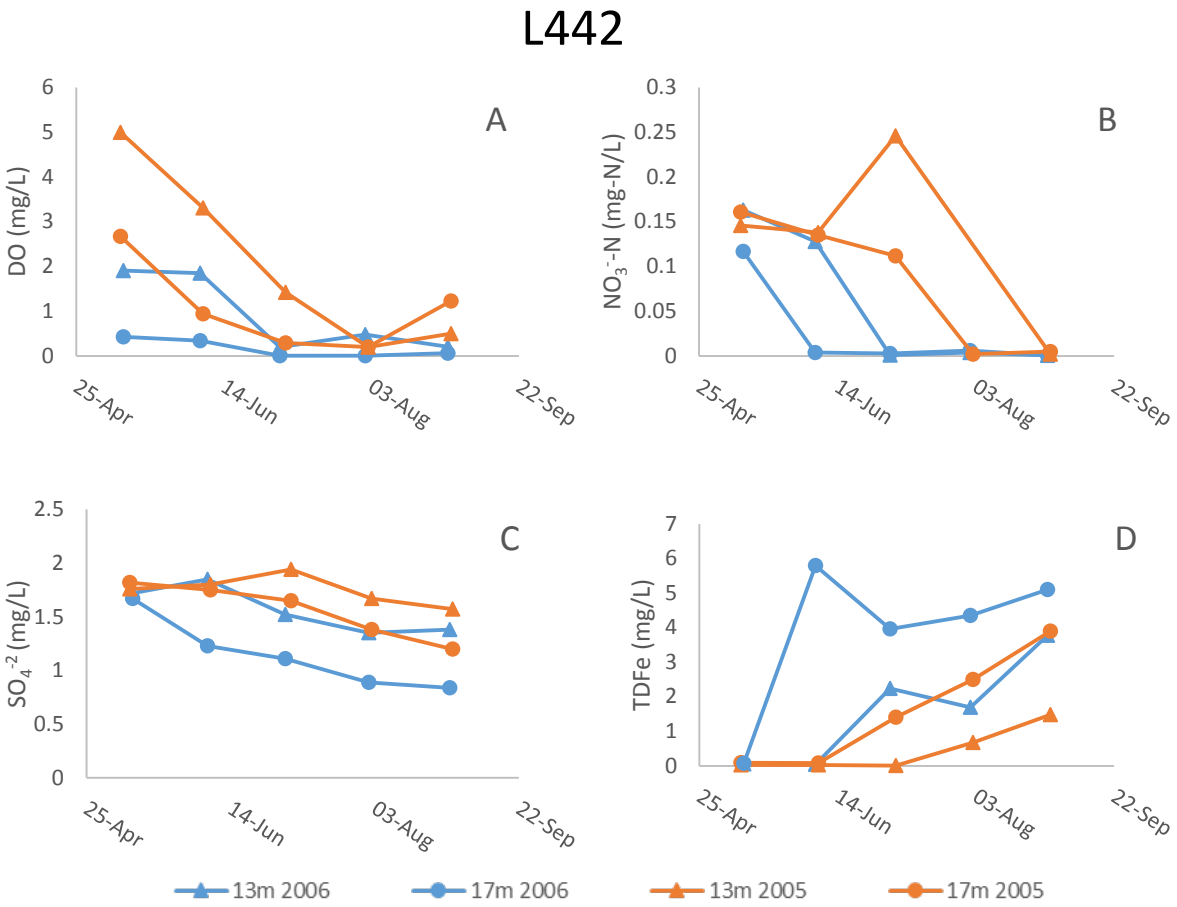

Figure 2.7 L442 13 m (triangles) and 17 m (circles) hypolimnetic concentration trends of (A) O_2, (B) NO_3^-, (C) SO_4^{2-} and (D)TDFe from May to September of both 2005 (organge) and 2006 (blue).

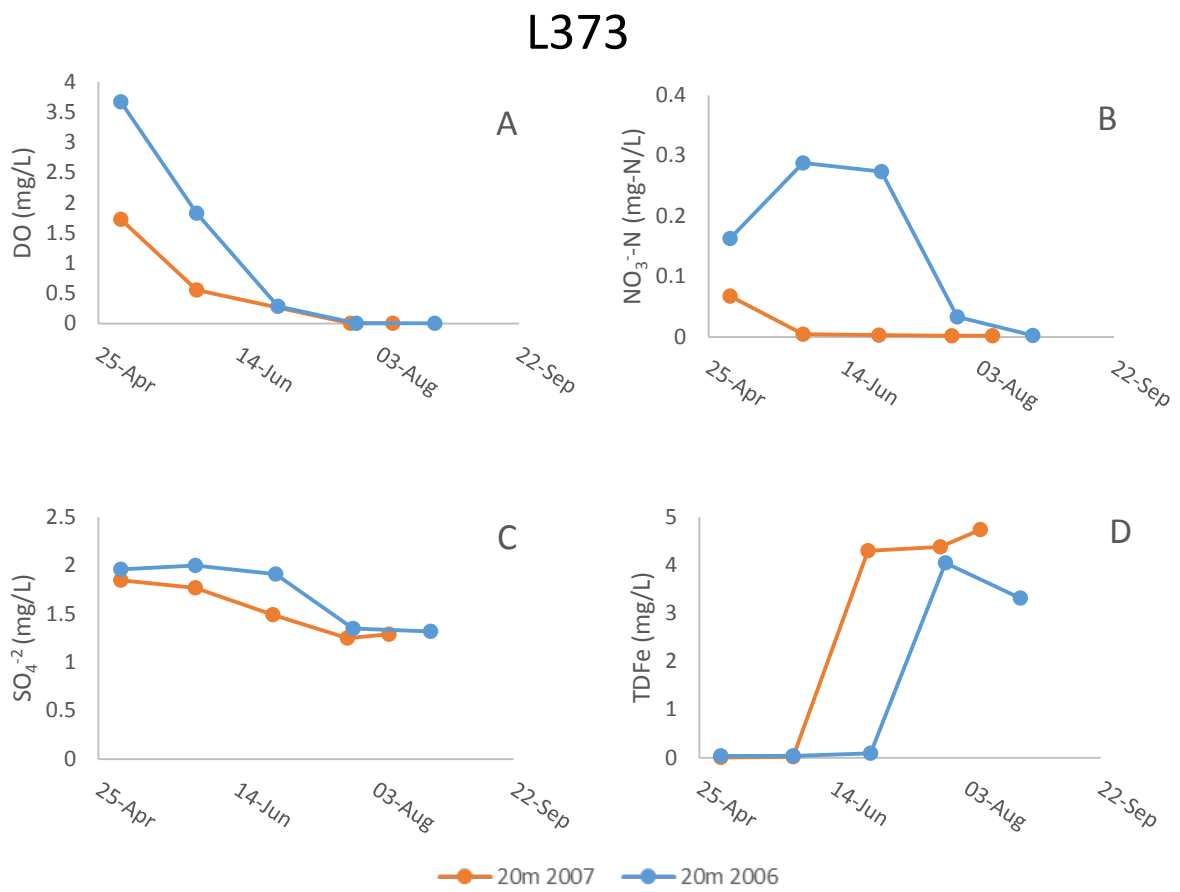

Figure 2.8 L373 20 m hypolimnetic concentration trends of O_2, NO_3^-, SO_4^{2-} and TDFe from late spring to early fall of 2006 and 2007.

L373 was only sampled at a depth of 20 m in the hypolimnion in 2007 and 2006. O_2 concentrations were initially higher (3.67 mg/L) in 2006 than in 2007 (1.73 mg/L) but both years reached 0.29 mg/L by 48 days after initial sampling (Figure 2.7). In 2006, NO_3^- concentrations increased from 0.16 mg-N/L to 0.29 mg-N/L and appear to remain constant until 48 days when O_2 was depleted at which point it decreases to 0.03 mg/L. In 2007, NO_3^- concentrations start low at 0.068 mg-N/L and reaches 0 mg/L by 20 days. SO_4^{2-} concentrations decreased by 0.61 mg/L and 0.6 mg/L in 2006 and 2007. Fe concentrations started at 0 mg/L and increased to 4.3 mg/L and 4.0 mg/L in both 2007 and 2006. Fe release began earlier in 2007 than in 2006 but both increased at roughly the same rate. In 2007 after Fe reached 4 mg/L

it remained constant for 27 days and then showed a minor increase where, in 2006, Fe concentrations decreased. At 17 m, in 2006, Fe release occurs immediately after initial sampling. At 13 m and 17 m, in 2006 and 2005 respectively, Fe release is delayed until 26 days after initial sampling. While NO_3^- concentrations are higher at 17 m in 2005 than at 13m in 2006, NO_3^- concentrations both drop below 0.15 mg-N/L at the same time, 26 days after sampling. Fe release at 13 m in 2005 occurs later than at the other depths and years due to a large increase in NO_3^- from 0.14-0.25 mg-N/L between 26 and 53 days after sampling.

2.3.2 Net Rates of Biogeochemical Processes

Sturgeon Bay

The rates of consumption of O_2, NO_3^- and SO_4^- and the rate of Fe accumulation observed in Sturgeon Bay at 10 m and 12 m were drastically different. The rate of O_2 consumption at 12 m is 30 ± 6.7 mg/m^2/day as opposed to 1014 mg/m^2/day at 10 m. Similarly, differences in Fe release rates between depths are observed with 66 ± 2.7 mg/m^2/day at 12 m depth and 719 ± 115 mg/m^2/day. Consumption and release rates of all redox species at 12 m are relatively consistent from 2014-2015. At 10 m O_2 and NO_3^- consumption rates appear to vary greatly from 2014 to 2015 with the rate of O_2 consumption increasing by 418 mg/m^2/day, NO_3^- rate constant decreased by 0.014 day^{-1}. However, the rate of Fe release and SO_4^{2-} consumption were similar in both years. Fe release varied little, from 719-717 mg/m^2/day, for 2014 and 2015 and the SO_4^{2-} consumption rate constant only increased by 0.004 day^{-1} (Table 2.4).

Deep Bay

At 12 m depth the rates for O_2, SO_4^{2-} and Fe increased from 2014 to 2015 while the rate of NO_3^- consumption decreased. At 16m the rates of O_2 and NO_3^- consumption decreased while the rates for SO_4^{2-} and Fe reduction increased. Changes in Deep Bay were not a large as those observed in Sturgeon Bay except for the Fe release rate at 16 m changing from 47 ± 8.5 mg/m^2/day to 365 ± 14 mg/m^2/day. SO_4^{2-} reduction rate constants in Deep Bay are significantly lower than in Sturgeon Bay (0.028 day^{-1} vs. 0.002 day^{-1} at bottom and 0.013 day^{-1} vs. 0.009 day^{-1} above the bottom) while Fe release rates, at the bottom depths, are higher (Table 2.4).

ELA

L373 rates were only calculated at 18 m (corresponding to a 2 m depth from 18 m-20 m) depth since that was only depth in the hypolimnion that data was available. The rate calculated for L373 in both 2006 and 2007 are similar to those calculated in both Sturgeon Bay and Deep Bay with the exception that NO_3^- consumption rates are higher in L373 than the Georgian Bay sites (Table 2.5).

L442 shows little O_2 consumption at 15 m compared to other sites but NO_3^- consumption rates are similar to those calculated for 18m in L373. Fe release rates at 15m in L442 are similar to those observed for the bottom depths of both Sturgeon Bay and L373 but at 13m rates are much lower than both Sturgeon Bay at 10m and Deep Bay at 16m. SO_4^{2-} reduction is similarly low in L442 as in L373 and Deep Bay (Table 2.5).

Table 2.4 Reduction rates and rate constants from multiple years and depths for Sturgeon Bay (SB), Deep Bay (DB), Lake 373(L373) and Lake 442 (L442). Rates are normalized to sediment surface area.

	SB 2014		SB 2015		DB 2014		DB 2015		L373 2006	L373 2007	L442 2006		L442 2005	
	12m	**10m**	**12m**	**10m**	**18m**	**16m**	**18m**	**16m**	**18m**	**18m**	**15m**	**13m**	**15m**	**13m**
O_2 (mg $m^{-2}day^{-1}$)	30	1014	45	1432	41	149	78	140	107	82	10	140	46	120
NO_3^- (day^{-1})	0.047	0.043	0.049	0.035	0.069	0.037	0.026	0.027	0.085	0.096	0.069	0.039	0.077	0.07
SO_4^{2-} (day^{-1})	0.028	0.009	0.036	0.013	0.002	0.003	0.003	0.009	0.002	0.003	0.006	0.003	0.005	0.003
Fe (mg $m^{-2}day^{-1}$)	66	719	55	717	151	47	174	365	59	78	57	87	51	50

Table 2.5 Initial concentrations (mg/L) for each redox species for each iteration of the redox model.

	Initial Concentrations Used to Run the Model													
	SB 2014		**SB 2015**		**DB 2014**		**DB 2015**		**L373 2006**	**L373 2007**	**L442 2006**		**L442 2005**	
	12m	**10m**	**12m**	**10m**	**18m**	**16m**	**18m**	**16m**	**18m**	**18m**	**15m**	**13m**	**15m**	**13m**
O_2	1.22	2.05	1.97	3.21	4.21	4.66	3.52	4.02	3.67	1.73	0.43	1.91	2.67	5
NO_3^-	0.26	0.16	0.16	0.1	0.14	0.19	0.13	0.2	0.16	0.07	0.12	0.16	0.16	0.15
SO_4^{2-}	4.4	5.16	3.5	3.5	5.1	5.1	4.4	4.5	1.96	1.85	1.67	1.72	1.82	1.76
Fe	0.15	0.15	0.29	0.2	0.16	0.1	0.3	0.268	0.04	0.01	0.07	0.05	0.09	0.02

2.3.3 Application of the Model

Sturgeon Bay

The model performs well in predicting the timing of Fe release at both 10 m and 12 m for both 2014 and 2015 in Sturgeon Bay. At all depths, in both years, Fe release was predicted within 5 days of field observation. However, the model performs poorly in predicting end of summer concentrations in 2014 at both depths. At 12 m the end of summer concentration was 1.6 mg/L lower than observed in field and, at 10 m, end of summer concentrations were under predicted by 1.4 mg/L (Figure 2.9).

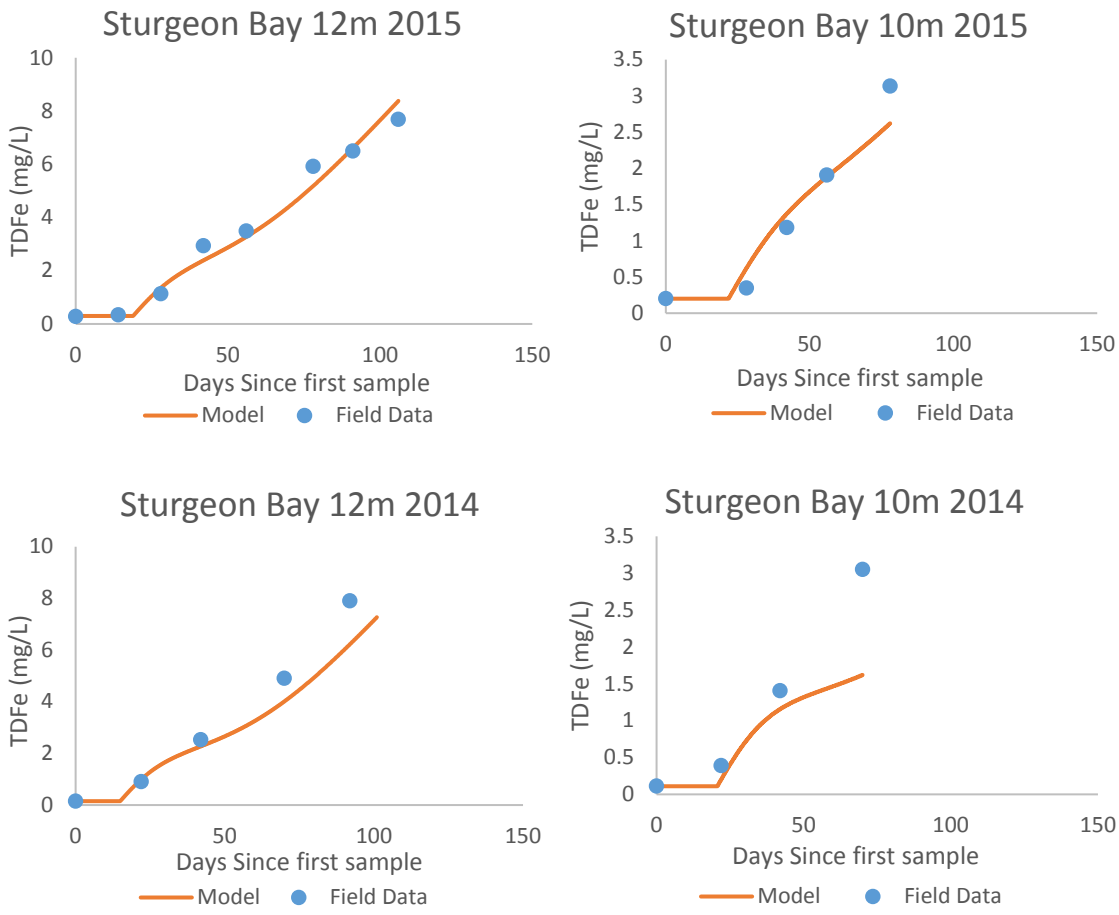

Figure 2.9 Field data of Fe concentrations at 12m and 10m depth in Sturgeon Bay (points) and model curves (solid lines) for the years 2014 and 2015. Plots for 2015 constructed using field data used to fit the model. ($RMSE_{201512m}$= 0.42 mg/L, $RMSE_{201510m}$= 0.28 mg/L, $RMSE_{201412m}$= 0.90 mg/L, $RMSE_{201410m}$= 0.73 mg/L, $E_{201512m}$= 0.96, $E_{201510m}$= 0.94, $E_{201412m}$= 0.81, $E_{201410m}$= 0.90).

Deep Bay

The model, when ran using Deep Bay values for 2014, better predicts Fe concentrations at 18 m than it does at 16m ($E_{201418m} = 0.78 > E_{201416m} = 0.48$). The timing of Fe release is predicted to within 10 days in all cases except at 18 m in 2014. At 16m depth the model under predicts end of summer Fe concentrations (Figure 2.10).

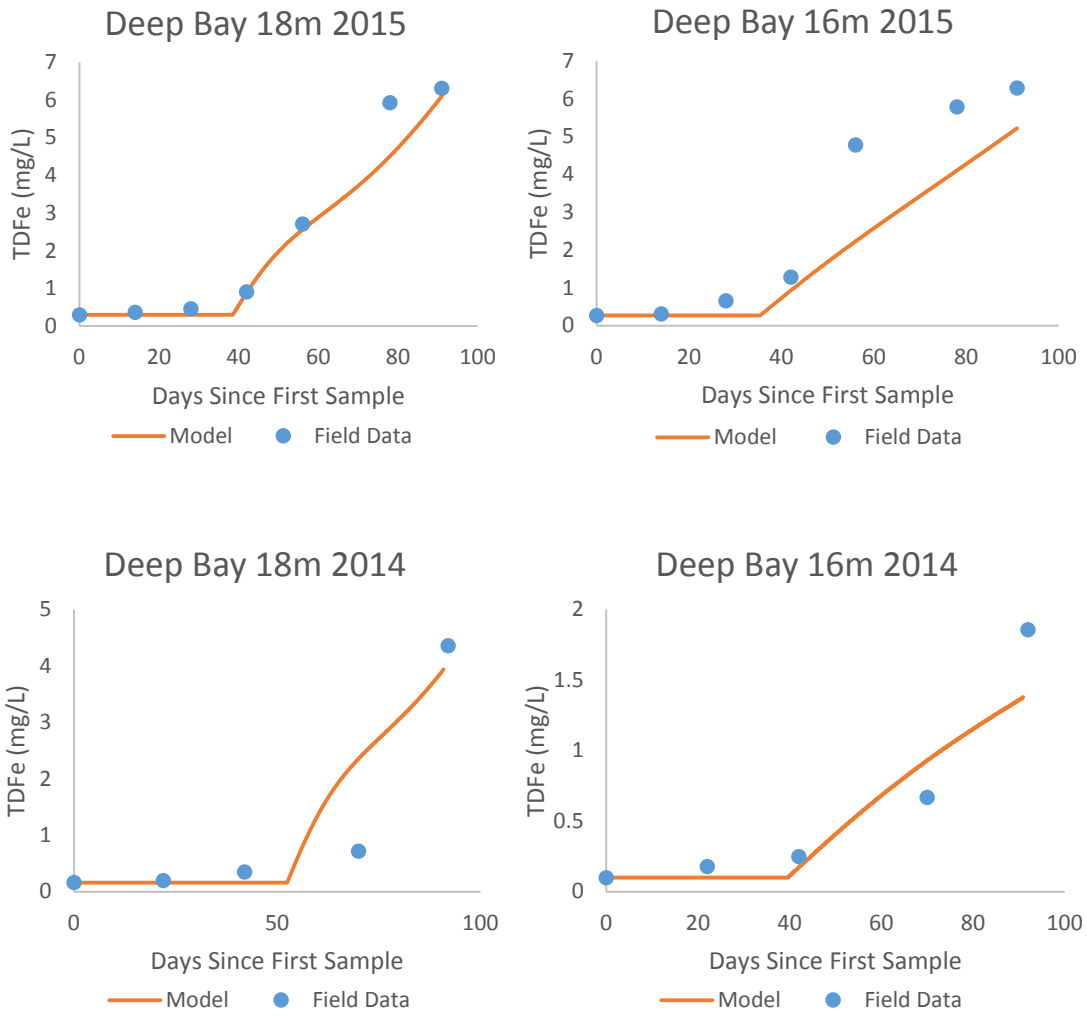

Figure 2.10 Field Data collected from both 16 and 18m from Deep Bay in 2014-2015 plotted against model output. ($RMSE_{201518m}$=0.55, $RMSE_{201516m}$=1.24, $RMSE_{201418m}$=0.76, $RMSE_{201416m}$=0.47, $E_{201518m}$=0.95, $E_{201516m}$=0.76, $E_{201418m}$=0.78, $E_{201416m}$=0.48).

Lake 373

The model, when fit to L373 2007 field data, shows good fit to the field data collected in 2006, accurately predicting the end of summer concentration of TDFe and predicting that TDFe would remain low until 56 days after sampling (Figure 2.11). The RMSE of the 2006 data was calculated to be 1.28 mg/L.

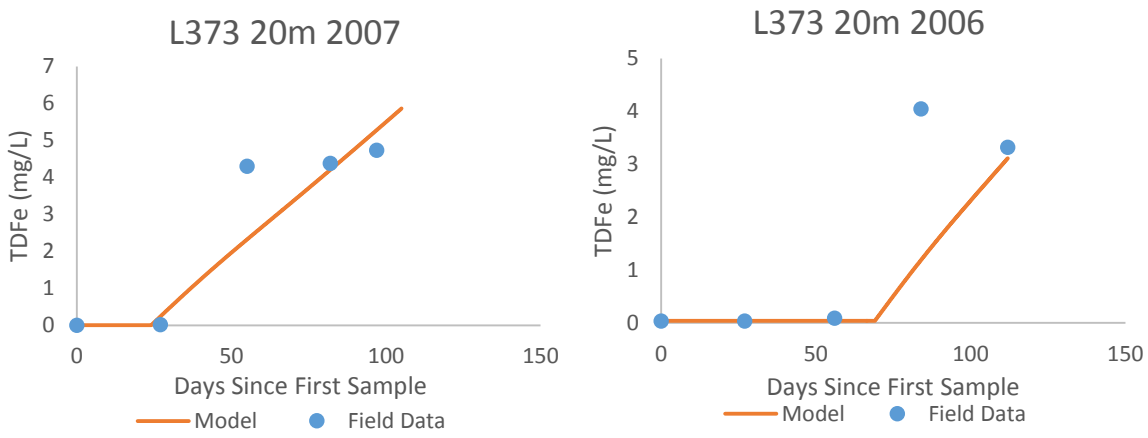

Figure 2.11 Field data from L373 at 20m in both 2007 and 2006 plotted against model output. 2007, the year that the field data used to determine rates shows a stronger correlation than 2006. ($RMSE_{2007}$= 0.92, $RMSE_{2006}$= 1.28, E_{2007}= 0.82, E_{2006}= 0.72)

Lake 442

In Lake 442, in 2005, Fe increase was more consistent and the model has a good fit with concentrations ($E_{200513m}$ = 0.97, $E_{200517m}$ = 0.85) and timing of Fe release (Figure 2.12). In 2006, Fe concentrations saw large spikes and decreases in TDFe concentrations which the model is unable to account for which is reflected in the negative Nash-Sutcliffe Coefficient (-0.11) calculated for the model at 17 m. Since both O_2 and NO_3^- concentrations are 0.4 and 0 mg/L during the anomalous Fe spike, and remain sufficiently low after, Fe would not likely increase that rapidly and then decrease a short period after and thus it is likely that this data point was a result of sampling error. By removing this data point an E of 0.93 and RMSE of 0.18 was calculated for the models fit to 2006 field data collected at 17 m. While a similar anomalous data

point was observed at 13 m of the same year, it was decided that this data point was not dissimilar enough to the next data point to justify its removal.

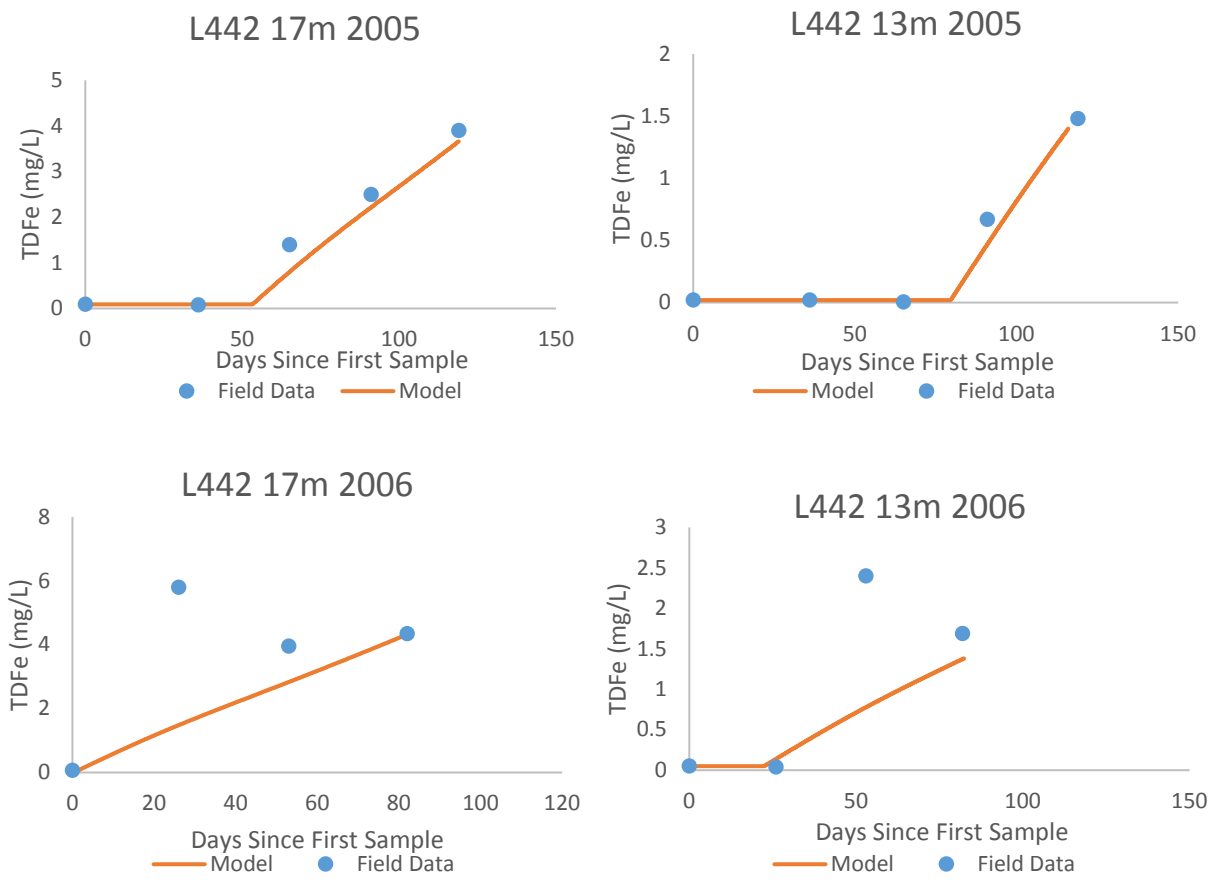

Figure 2.12 Field Data collected from both 13 and 17m from L474 in 2005-2006 plotted against model output. ($RMSE_{200513m}$=0.54mg/L, $RMSE_{200517m}$=0.10mg/L, $RMSE_{200613m}$=0.91mg/L, $RMSE_{200617m}$=2.57 mg/L, $E_{200513m}$=0.92, $E_{200517m}$=0.87, $E_{200613m}$= 0.41, $E_{200617m}$=-0.1).

2.4 Discussion

2.4.1 Rate Kinetics

In order to initialize the model, rate orders needed to be determined. Rate orders, such as 0^{th} order and 1^{st} order, are expressions of how the rate of a reaction changes over time relative to the concentration of the reactants. 0^{th} order reactions, by definition, are linear meaning that the

rate of consumption of reactants and production of products is constant at any concentration of reactants. Contrarily, the rate of change of the chemical species in question in a 1^{st} order reaction changes depending on the concentration. While initial rate orders were determined from results obtained from the field studies of Sturgeon Bay and Deep Bay conducted for this thesis, results from other research were used to justify the rate orders used.

Oxygen

O_2 consumption rates vary greatly (3.2-4500 $mg/m^2/day$) from system to system due to; organic matter availability, the redox environment and the physical mixing (movement of water through forces such as wind) conditions of a body of water (Santschi, 1989). However, the rate order of O_2 consumption is typically 0^{th} order unless a thick enough diffusion limited boundary layer is formed between the sediment and water due to the friction slowing the flow of water over the sediment causing a lack of turbulent mixing at the SWI. This process causes the main flux of O_2 to the sediment to be governed by diffusion, resulting in a first order rate for O_2 concentrations below 3mg/L (Hall et al., 1989). Without a closer study of the boundary layer between the sediment and the water column, it is impossible to determine whether or not the assumption that O_2 consumption follows 0^{th} order rate kinetics is correct. It is possible that, at the sampling resolution used here O_2 consumption rates appear to be linear relative to the consumption rates of SO_4^{2-} and NO_3^-. It is possible, that due to the sampling resolution, a period of rapid, first order O_2 consumption was missed, however there is no way to assess this based on that data available. Therefore, for the sake of the model developed here, assuming O_2 consumption is linear appears to be adequate for predicting the timing of Fe release to within 10 days.

NO_3^-

In the case of NO_3^-, reduction rates tend to follow first order rate kinetics when NO_3^- concentrations are near or below 0.14 mg-N/L (Knowles, 1982). NO_3^- Concentrations observed in both Deep Bay and Sturgeon Bay in early May (0.13 mg-N/L and 0.17 mg-N/L respectively) are close to this value, suggesting that assuming a first order rate equation is appropriate for modelling NO_3^- consumption near the SWI. The likely cause for this rate order is due to the high consumption rate of NO_3^- matched with the relatively low concentrations available at the SWI. This results in the consumption rate of NO_3^-, at the sediment water interface being driven by diffusion and thus affected by the concentration gradients present at a given time (Santschi, 1989; Rudd et al., 1986).

Sulphate

In the model proposed here it was assumed that SO_4^{2-} concentrations in the overlaying water played a major role in controlling Fe release from sediments. While the assumption that SO_4^{2-} reduction rates could be approximated using first order rate kinetics appears to be valid (Rudd et al., 1986), the pool of SO_4^{2-} that has the largest impact of Fe reduction is more likely to be in the pore water and not the overlaying water column. Since SO_4^{2-} reduction typically occurs deeper in the sediment, away from the SWI (Santschi, 1989), it is not likely that the concentrations of SO_4^{2-} in the water column above the sediments play a major role in suppressing Fe release. Once all other electron acceptors are depleted SO_4^{2-} in the pore water will be reduced. The H_2S produced will diffuse upward toward the SWI and interact with Fe(II) precipitating Fe-S compounds. Therefore, as SO_4^{2-} reduction occurs away from the SWI, H_2S may build up in deeper sediments while, at the SWI, Fe(III) reduction is suppressed due to the presence of O_2 and NO_3^-. This built up H_2S may then diffuse toward the SWI and suppress the release of Fe(II) once

Fe(III) reduction occurs. However, further research observing SO_4^{2-} rates in the sediment of Sturgeon Bay and Deep Bay would be required to modify the model appropriately.

Fe

In literature Fe release rates are reported as mg/m^2/day which implies that Fe release follows a linear rate, however no explicit mentions of linearity were found. To examine the hypothesis that Fe release is indeed constant after the absence of other electron acceptors, Fe concentration data from two lake scale studies were plotted and a linear regression was conducted on all plots (Foy, 1985; Søndergaard, 2000). For both cases, Fe release was shown to follow a linear equation with R^2 values greater than 0.95.

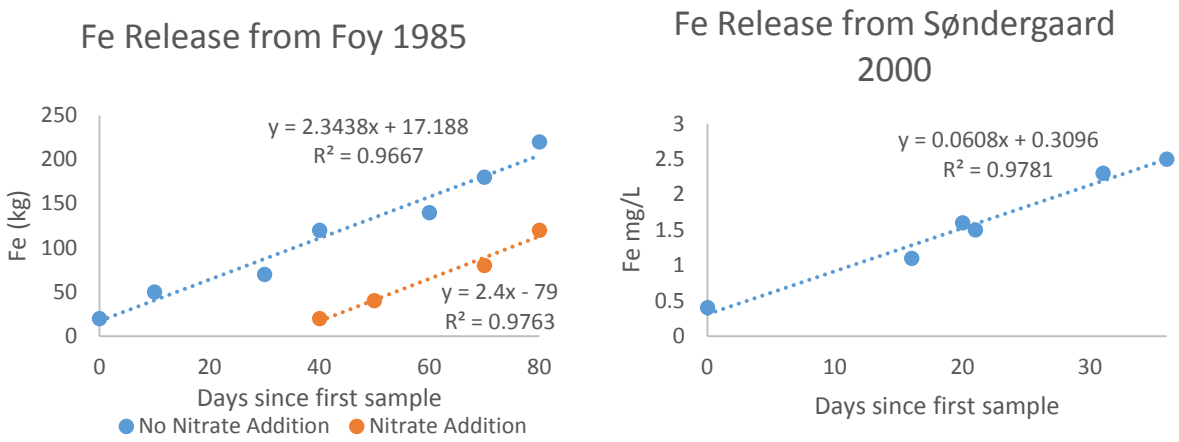

Figure 2.13 Fe plotted against days since first sample for data collected from Søndergaard, 2000 and Foy 1985. Linear trendlines show good correlation (R^2>0.96) to field data.

The formation of a thick boundary layer of stagnant water at the SWI can limit the flux of Fe to diffusion between the sediment and the water column. Concentrations of reducible Fe in sediments at Sturgeon Bay are likely high enough that any change in pore water Fe concentration may be negligible. In Sturgeon Bay, reducible Fe accounts for approximately 1.2 % of sediment

by dry weight (Verschoor, 2016). Assuming most of the Fe released from sediment originates from the top 2cm, and using the surface area of the last meter of the hypolimnion in Sturgeon Bay, this equates to $5.73x10^{10}$ mg Fe. With an average Fe reduction rate of 65 mg/m^2/day this Fe would persist for roughly 10 years, much longer than the typical stratification period of approximately 100 days. Additionally, this mass of reduced Fe would precipitate during turnover, returning it to the sediment where it can be reduced again the follow season. Thus, it is unlikely that rates would decrease or ever reach zero over the 100 days of stratification due to an absence of reducible Fe.

2.4.2 Rates

Rates in the Bottom Meter of the Hypolimnion Between Years

The bottom-most meters of the hypolimnion were the main focus while constructing this model. One reason for this is that, during stratification, the bottom meters of a lake are the most likely to consistently go anoxic from one year to the next and, as a result, would be where a parsimonious model based on redox reactions would be most useful and is where this type of model could be tested. While some natural variation in the rates was expected, the rates observed appear to be relatively consistent from year to year within the same lake. Fe release rates varied the least with an average variation of 16% from one year to the next at the deepest location across all lakes. NO_3^- has the second least variation between its consumption rate constants at 22%. SO_4^{2-} and O_2 rates varied the most, with differences in rates of 32% and 42% between years respectively. However, it is important to note that a majority of rate constants of SO_4^{2-} consumption all fell into a range of 0.02-0.06 day^{-1} so even a small change in rate constants between years represents a large percentage change.

The low differences in rates between years for both Fe and NO_3^- suggests that assuming rates are constant between years is adequate. In addition the large variation in DO consumption rates may explain why the model is only able to predict the timing of Fe release from the sediment after anoxia to within 10 days. Since DO is modeled using a linear rate an increase in the consumption rate by 30% would decrease the time after anoxia at which Fe would begin to release by the same factor.

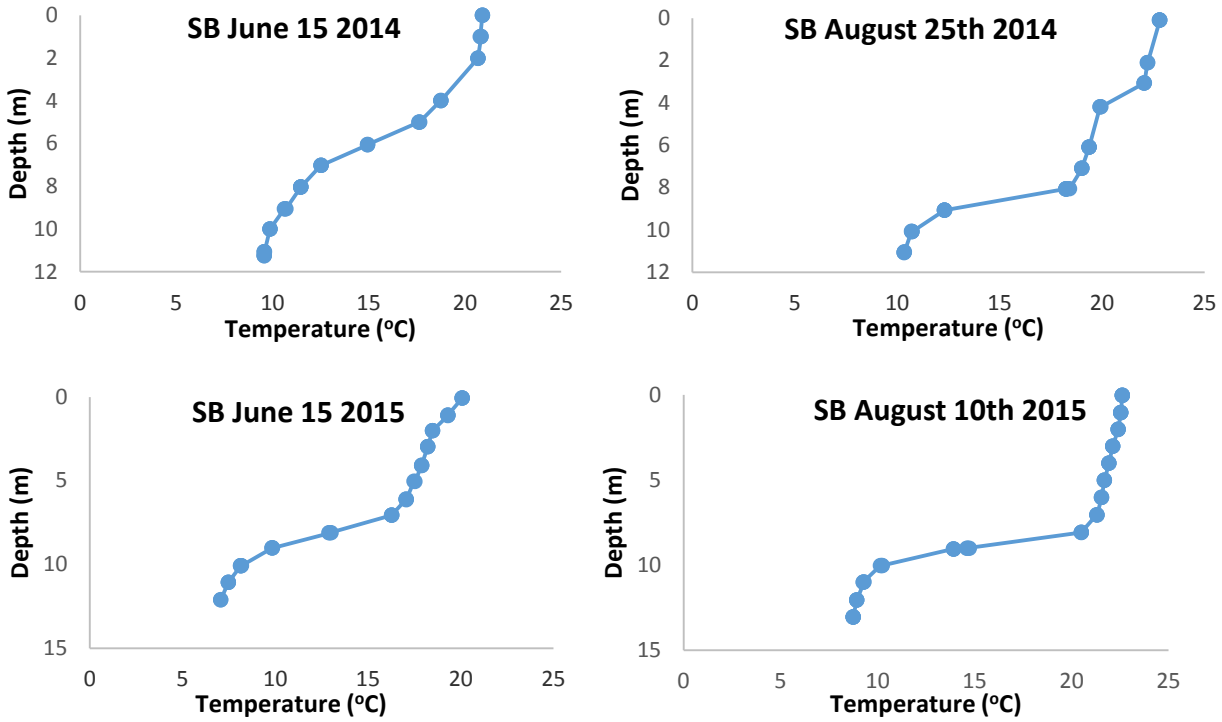

Figure 2.14 Temperature profiles taken at the start and just before the end of stratifiaction in Sturgeon Bay in 2015. Profiles show that below 10m SB was stratified through the sampling season in both 2014 and 2015.

Comparing Rates Between sites

The most consistent rates are the reduction of Fe and NO_3^- which, when averaged across all sites studied for the year used to fit the model and then compared to the average of the other years, vary by approximately 21 % and 25 %, respectively, between years. Less consistent are

the reduction of O_2 and SO_4^{2-} for which the average variations are 42 % and 34 %, respectively. Some of this variation could be due to lack of sampling resolution. In this study only eight sets of data were collected over the stratification period and, of those, only 3 to 4 points were used in the calculation of rates. Additionally, rates observed in Sturgeon Bay are different than the rates observed in Deep Bay which are different from those observed in L373 and L442. This natural variation in rates demonstrates that it is necessary to initialize the model using data from the lake of interest.

Variation of Rates between Depths

In order to assess the ability of the model to predict Fe release at other depths in the hypolimnion, complete lake profiles are required as rates can change drastically from one depth to another. For instance, in Sturgeon Bay Fe release at 12 m in 2015 was 72 mg/m^2/day whereas at 10m it was 1010.1 mg/m^2/day (Table 2.4). While the volumetric rate may be similar between depths, the sediment surface area : volume of these discrete layers differs. As a result, rates measured at one depth are not appropriate for use at all depths. Of the sites studied, those that are connected to Georgian Bay exhibit the largest discrepancy in all rates based on depth compared to the more hydrologically isolated Lake 373 and Lake 442. This suggests that some factor of mixing between Georgian Bay and both Sturgeon Bay and Deep Bay may be disturbing the stratification of these lakes. If that is the case it is possible that bottom waters with high concentrations of Fe and low concentrations of NO_3^-, O_2 and SO_4^{2-} are being mixed into the upper layers later in the season resulting in an apparent increase in Fe release and NO_3^-, O_2 and SO_4^{2-} consumption.

Rates Observed In Literature

Reported O_2 consumption rates at the SWI in lake scale experiments in literature range from 44 -1500 mg/m^2/day, while Fe release rates range from 9-2240 mg/m^2/day (Table 2.6). The O_2 consumption rate measured in Sturgeon Bay in 2015 is 30 mg/m^2/day which is 14.8 mg/m^2/day less than the lowest rate found in literature and 11 mg/m^2/day lower than observed in Deep Bay. Alternatively, Fe release rates, in all four lakes in this study (Sturgeon Bay, Deep Bay, L442 and L373), are found in the middle of the range of Fe release rates observed in other lakes. The majority of the O_2 consumption rates found in literature are over 300 mg/m^2/day range from 348.8-1500 mg/m^2/day. Both Sturgeon Bay and Deep Bay have O_2 consumption rates an order of magnitude lower than the lower end of this range at 30 and 41mg/m^{2}L respectively. Conversely, a majority of the Fe release rates fall in the range of 40-80 mg/m^2/day with Sturgeon Bay laying at the upper end of this range (66 mg/m^2/day) and Deep Bay exceeding it (151 mg/m^2/day). As a result, both Sturgeon Bay and Deep Bay have high Fe release : O_2 consumption ratios relative to the literature values (Table 2.6). Sturgeon Bay has a ratio of 2.2 and Deep Bay has a ratio of 3.7 while the ratios for the lakes studied in other literature fall in the range of 0.01-0.5. This suggests that in Sturgeon Bay and Deep Bay, managing anoxia through aeration, to prevent internal loading of Fe, may be an efficient method since the O_2 consumption rate is low, meaning any increase in O_2 concentration would have a long lasting effect. However, once O_2 is depleted, Fe will accumulate in these lakes at a high rate relative to rates observed in other lakes, potentially promoting cyanobacteria dominance of the phytoplankton biomass.

While most Fe release rates range from 30-60 mg/m^2/day, there does not appear to be a clear link between geography and rates. For example, while the rates for all 3 sites located at ELA (L227, 373 and 442) all have rates close to 60 mg/m^2/day, rates from the three Swiss lakes:

Pfaffikersee, Tulersee and Murtensee have rates of 56, 37 and 13 mg/m^2/day, respectively (Müller, 2012). Additionally, Sturgeon Bay and Deep Bay, both located along the east shore of Georgian Bay have rates that differ by almost 100mg/m^2/day. Similarly, the O_2 consumption rates for lakes located in close geographic proximity have rates that can differ by up to 900 mg/m^2L. While some rates appear to be similar, only differing by a factor of two (Tulersee and Murtensee), this would alter the timing of Fe release predicted by the model as well as the end of summer estimated Fe concentration by the same factor since the rates of both O_2 and Fe are based on linear equations. This means that it is not necessarily geographic location that governs the release rate of Fe or the consumption rate of O_2, but possibly the sediment type present in each lake. As such, it is not advised to use the model presented here assuming that rates measured at a similarly sized lake, located near a lake of interest, has similar rates. Instead, collecting data to determine the specific Fe release and O_2 consumption rates for said lake is required.

2.4.3 Predicting Timing of Fe Release

Georgian Bay

In the Georgian Bay sites, the model was able to predict the timing of Fe release to within an average of 10 days. When the model was applied to Sturgeon Bay for the years 2014 and 2012 the timing of Fe release was predicted to occur within 8 days of when Fe accumulation was observed in field samples (Fig. 2.9). However, the model was only able to predict Fe release to within 12 days when applied to Deep Bay in 2012 and within 2 days in 2014 (Figure 2.10). The discrepancies between year and site are likely due to natural variability in rates as well as the difference in sampling frequency. In 2014 samples were taken less often so the resolution may be too coarse to observe similar changes. Since the model uses a single year of data to determine

rates any changes in rates observed in field in subsequent years will result in deviations from the model prediction. However, despite these differences, these results imply that a simple redox model, initiated with a single year of intensive sampling data, is able to approximate how many days after a single sampling trip, in early May, that Fe release can be expected to occur in other years.

ELA

The best prediction of Fe release timing was L442 in 2006 with Fe release occurring at the same time as predicted at 17 m and 6 days later than predicted at 13 m. In Lake 373 in 2006 Fe release occurred 14 days earlier than the model predicts. Overall, Fe release is predicted to within 7 days on average in the ELA lakes studied here.

Table 2.6. O_2 and SO_4^{2-} consumption rates and Fe release rates at the SWI observed in lake scale experiments. The wide range of O_2 and Fe values show that there is a natural variability in rates between lakes, locally (L373 and L442) and globally

Lake	O_2 Consumption ($mg/m^2/day$)	Fe Release ($mg/m^2/day$)	SO_4^{2-} Rate Constant (day^{-1})	SO_4^{2-} Consumption ($mg/m^2/day$)	Geographic location	Sample location	Source
Sturgeon Bay	30	66	0.036*		Ontario	Hypo-	This research
Deep Bay	41	151	0.006*		Ontario	Hypo-	This research
Lake 373	107	59			Ontario	Hypo-	This research
Lake 442	1010	57			Ontario	Hypo-	This research
Sagamore				3.01	New York	Epi-	Rudd et al., 1986
Big Moose				18.4	New York	Epi-	Rudd et al., 1986
Woods				16.7	New York	Epi-	Rudd et al., 1986
Gull Pond	44.8				Cape Cod	Hypo-	Rich, 1979
Hathaway Pond	108.8				Cape Cod	Hypo-	Rich, 1979
Mares Pond	348.8				Cape Cod	Hypo-	Rich, 1979
Puget Sound		41			B.C		Murray and Gill, 1978
Turlersee	600	37			Switzerland	Hypo-	Müller, 2012
Pfaffikersee	840	56			Switzerland	Hypo-	Müller, 2012
Murtensee	1030	13			Switzerland	Hypo-	Müller, 2012
Baldeggersee	1170				Switzerland	Hypo-	Müller, 2012
Sempacheree	1500				Switzerland	Hypo-	Müller, 2012
White Lough	1300	77.4			N.Ireland	Hypo-	Foy , 1986
Lake 227		62			Ontario	Hypo-	Cook, 1984
Lake Erie	460				Ontario	Hypo-	Bouffard, 2013
Salmon Lake		212			Michigan	Hypo-	Amirbahman, 2003
Webber Pond		190			Michigan	Hypo-	Amirbahman, 2003
Sebasticook		132			Michigan	Hypo-	Amirbahman, 2003
Island Pond		45			Michigan	Hypo-	Amirbahman, 2003
Keoka Lake		11			Michigan	Hypo-	Amirbahman, 2003

2.5 Summary and implications

A simplified model of Fe release from hypolimnetic sediments in a lake, based on data during stratification was developed. This model assumed that each depth in the hypolimnion acts as a closed system and, that simplified redox reactions govern Fe release. When fit to field data from a single year, the model accurately (mean E= 0.73) and with small error (mean RMSE 0.76 mg/L) predicts Fe release and accumulation consistent with data collected from all field sites. The model is also applicable to depths above the bottom 2 m, however, each depth must be considered its own system and rates must be calculated for each system independently due to the wide range of rates between depths and because the model separates depths with no diffusive or advective transfer of material between the layers. The rates calculated from 2015 field data at 12 and 10 m for O_2, NO_3^- and SO_4^{2-} consumption were a good approximation of year to year rates for Sturgeon Bay. Applying initial conditions of 2014 to the model resulted in an accurate prediction of the timing of Fe release in each scenario for Sturgeon Bay. However, this model is not appropriate for all lakes. When the model is applied to data from Deep Bay there is an over estimation of the Fe accumulation in the early stages of Fe release. More research is required to distinguish what characteristics of Deep Bay may hinder the applicability of the model and if the model can be adjusted to compensate for these discrepancies. While the model does not work as intended for Deep Bay, the model has potential use as a relatively quick, cost effective method to predict O_2, NO_3^- and Fe concentrations over the course of a summer and could be used to make decisions surrounding timing of management implementation, should an effective strategy for controlling cyanobacteria be developed that is based on controlling the redox conditions at the sediment water interface of the anoxic zone.

Chapter 3: The Role of Nitrate on the release of Fe during Sediment Incubations

3.1 Introduction

N is an essential nutrient for all life on earth. The largest global pool of N is in the atmosphere as gaseous N_2. N_2 is an inert gas and only enters the biosphere once converted to reduced N. Some organisms can fix atmospheric N_2 converting it to NH_3 which is biologically available to other organisms and can in turn be converted to many N compounds including NH_4^+, NO_2^- and NO_3^-. However, some cyanobacteria species have the ability to fix atmospheric N_2, giving them an advantage over other phytoplankton in water bodies with low bioavailable N concentrations.

In addition to being used as a nutrient to grow biomass, NO_3^- also plays a key role in controlling the redox status at the SWI. When lakes experience thermal stratification, vertical mixing is greatly hindered, reducing the flux of oxygen from the atmosphere to the hypolimnion. This reduced flux of O_2 to the hypolimnion, coupled with respiration at the sediment water interface, will result in an anoxic hypolimnion should the O_2 demand of the sediment be high enough to counteract the diffusion of O_2 from the atmosphere. NO_3^- is a strong oxidizer (electron acceptor) which is consumed after the hypolimnion becomes anoxic. The presence of NO_3^- at the SWI prevents other electron acceptors at the sediment surface from being reduced because electron acceptors that are more energetically favorable, such as NO_3^- are reduced first following the redox ladder (Figure 1.3). The redox ladder is a conceptual model that orders electron acceptors based on the Gibbs free energy of a reaction. Reduction (respiration) of O_2 is the most energetically favourable reaction followed immediately by NO_3^-. This sequential reduction of

electron acceptors means that NO_3^- is important to consider when studying biogeochemical cycles that govern hypolimnetic chemistry.

Anthropogenic activities, such as agriculture and waste water are the largest sources of NO_3^- to surface waters. In the case of agriculture, the ability to fix N_2 industrially promoted a large increase in use of NH_4NO_3 fertilizer. The Haber-Bosch process converts atmospheric N_2 to ammonia (NH_3) and, since NH_3 was easy to manufacture, $NH_4NO_3^-$ fertilizers were also easier to produce and more affordable (Galloway, 2008). For example, in the Grand River Watershed, located in southern Ontario, N loading to surface waters between 1951 and 1986, due to fertilizer application and subsequent run off, increased from 2 kg N/ha/year to 27 kg N/ha/year and has remained relatively stable since that time (Zhang, 2016).

Another source of N loading to lakes is through atmospheric deposition of nitrogen oxides (NOx). Over the last 100 years, in the Grand River Watershed, atmospheric N deposition has increased from 14 kgN/ha/year to 25 kgN/ha/year (Zhang, 2016). This increase was likely to combat the increase in NOx emission from fossil fuel burning. Since the Canada-United States Air Quality Agreement was put in place in 1991 to limit NO_x and SO_x emissions, atmospheric deposition of N has been decreasing. In Central Ontario, atmospheric deposition can represent 35-75% of N loading (Molot and Dillon, 1993) and changes in deposition could affect the biogeochemical cycles of lakes in these areas.

P is also a key element in the production of biomass and is typically the limiting nutrient in lakes (Kalff, 2003). In 1972 the Great Lakes Water Quality Agreement (GLWQA) was enacted due to rising occurrence of algal blooms. In 1978 target concentrations of P were established for all the Great Lakes as well as individual goals for each basin of Lake Erie. P targets in both Lake Superior and Lake Huron were 5 µgP/L. In Lake Michigan the target value

was 7 µgP/L while Lake Ontario had a target of 10 µgP/L. Targets for Lake Erie differed depending on the basin. Both the Central and Eastern basins were given targets of 10 µgP/L however, the Western basin was given a target of 15 µg/L due the high level of P loading that occurs here (Dove and Chapra, 2015). Since the GLWQA set targets, P values have reached targeted values in Lake Erie (Scavia et al., 2014; Phosphorous Loading Targets. 2015, Dove and Chapra, 2015) and decreased past target values in all other Great Lakes (Dove and Chapra, 2015).

By increasing the N concentrations and decreasing the P concentrations in the lakes the N:P ratio of the lake water increases. It has been hypothesized that an increased N:P ratio reduces the risk of blooms dominated by N-fixing cyanobacteria and reduces biomass if P is reduced (Smith, 1983; Orihel, 2015). If the biomass is limited by bioavailable P instead of N, organisms that are unable to fix N_2 will be able to compete with N fixing cyanobacteria. Additionally, it has recently been hypothesized that Fe(II) may play a key role in promoting the dominance (defined in Molot. 2014 as > 50 % of phytoplankton biomass) of all species of cyanobacteria (Verschoor et al., 2017). Since cyanobacteria have higher Fe requirements than eukaryotes but are unable to utilize Fe(III) directly, the availability of Fe(II) is important to consider. The presence of NO_3^- at the sediment water interface of anoxic lakes prevents the use of Fe(III) as an electron acceptor because the reduction of NO_3^- occurs earlier in the redox ladder than the reduction of Fe(III). This prevents the accumulation of Fe(II) in the overlaying water column which potentially limits cyanobacteria growth which depends strongly on Fe(II).

Studies have shown that the addition of NO_3^- to a lake's hypolimnion can suppress the release of biologically important P, by preventing of Fe(III) reduction at the sediment water interface, into overlaying waters during stratification (Søndergaard, 2000; Schauser, 2006;

Beutel, 2016). These studies mainly focus on P, which is a critical nutrient that controls biomass accumulation in a lake, however, the results reported in these papers also suggest that the TN:TP and Fe(II) availability hypotheses for predicting cyanobacteria dominance may both be a result of the same factors. By increasing NO_3^- concentration in the lake, both the N:P ratio increases and the duration of Fe release from the sediment water interface decreases, which both result in a lower likelihood of cyanobacteria dominated blooms according to the Molot et al. (2014) hypotheses. This means that it is immensely important to examine the magnitude and duration of the effects that NO_3^- has on Fe(II) release from sediment.

The objectives of this chapter are to:

1. Test the response of Fe release from sediments to NO_3^- by manipulating the overlying water column NO_3^- concentration in bulk surficial sediment collected from a lake basin that experiences recurring blooms of cyanobacteria and;
2. Test the assumptions regarding rate equations made when constructing the conceptual and numerical model of a coupled Fe-NO_3^- system by manipulating the overlaying water NO_3^- concentrations

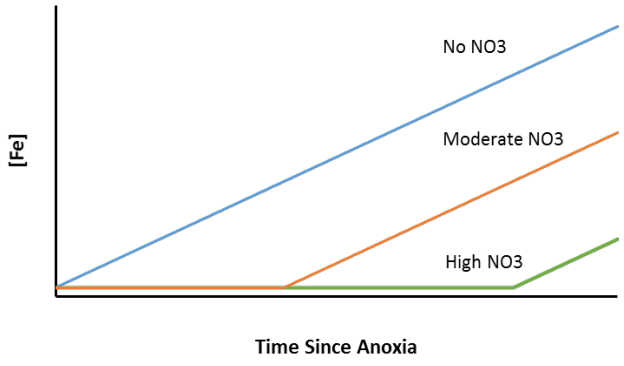

Figure 3.1: A schematic showing the expected effect of initial NO_3^- concentration on the timing and rate of Fe release from sediments.

3.2 Methods

3.2.1 Sediment Collection

Sediment was collected from deepest point in Sturgeon Bay, Ontario in the early spring of 2016. Sediment was collected in early May, prior to stratification, to ensure that bottom waters were oxic so that minimal reduction of Fe at the sediment surface had occurred before samples were collected for the incubations. Sediment cores were collected using a UWITEC gravity corer fitted with a 60cm long PVC coring tube. The top 5 cm (333 mL) of sediment were collected from each of 12 cores taken and stored in 1 L glass mason jars for a total of 4 L of sediment with overlying air in an attempt to maintain oxic conditions. Sediment was homogenized upon collection through vigorous agitation and then stored on ice for transport back to the University of Waterloo where the sediment samples were stored in the dark at approximately 6 ^{o}C.

3.2.2 Incubation Setup

Two liters each, of solutions with 1, 2 and 5 mg-N/L (low, med, high) of NO_3^- were created from a stock standard of $NaNO_3$ dissolved in DI. These solutions were bubbled with N_2 gas in a beaker until the O_2 concentration reached approximately 1mg/L. Three sets of seven (one set for each solution) 200 mL glass serum bottles were filled will 150 mL of the solutions. Wet sediment was re-homogenized and 50 mL of sediment was added to all serum bottles using a 60 mL syringe. The sediment was slowly injected to minimize suspension through the solution to limit mixing of pore water. To prevent oxygen from dissolving into the water from the headspace, the bottles were then pre-filled completely with the degassed solutions. Butyl rubber stoppers (Bell Co.®), pierced with a 22 gauge 1 ½" needle to equalize the pressure, were used to seal the bottles, after which the needle was removed. Stoppers and bottles were crimped together to ensure minimal atmospheric O_2 could enter during the incubations. Once all bottles were filled

and sealed, one bottle from each treatment was sampled immediately for O_2, NO_3^-, SO_4^{2-} and dissolved Fe concentrations. All other bottles were gently placed on their sides in a refrigerator at approximately 4 ^oC. Once per day all bottles were lightly agitated to allow some mixing at the SWI but not strongly enough to suspend sediment.

3.2.3 Incubation Sampling

The incubation set up was done in a sacrificial manner. All samples started incubating at the same time and the assumption is, that if all external conditions remained equal for the duration of the incubation, each sample would progress in tandem. Hence, sacrificing a single sample from each set at a specific time would mimic conducting an incubation in one bottle in which water would have to be replaced. Samples for the low and medium NO_3^- solutions were collected at t=0, 3, 6, 9 and 12 days after the experiment had begun with duplicate samples being collected on the 3rd and 9th days. For the high NO_3^- solution samples were collected at t=0, 4, 9, 13 and 23 days with duplicates collected on the 4th and 23rd days. This change in sampling protocol was to ensure that there would be a data point after NO_3^- has been sufficiently consumed. In order to keep samples as anoxic as possible during subsampling, two syringes were used to draw water from the bottles. The first 60 syringe was purged 3 times, and then filled, with N_2 gas. A 22 gauge, 1 ½" luer lock needle was attached to the syringe and used to puncture the stopper. A second 60 mL syringe was attached to a 3 way valve that had a needle and a smaller syringe with the plunger removed on the other 2 openings. The needle from this set up was inserted into the stopper and 60 mL of sample was pulled through into the syringe. The valve was set to close the opening the needle was attached to and sample was pushed up into the smaller syringe which contained a HACH O_2 probe. O_2 measurements were taken 3 times to ensure accuracy and the sample was pulled back into the large syringe. At this time the needle

was removed from the syringe and replaced with a 0.45 μm syringe tip filter. The valve was then turned to open the end with the syringe tip filter so sample could be passed through. Samples for anions and Fe were collected in 20 and 45 mL Nalgene bottles respectively. Fe samples were acidified to a pH of approximately 2 using nitric acid and both samples were refrigerated for later analysis.

Anion samples were analyzed on a Dionex IC-2000 at the University of Waterloo Environmental Geochemistry lab for NO_3^-, SO_4^{2-}, F^-, Cl^- and Br^- (DL= 0.05 ±0.02 mg/L). Dissolved Fe analyses were conducted at the Center for Cold Regions and Water Science on an ICP-OES. Data was reported as mg/L of analyte (error = ±0.06 mg/L DL= 0.1 mg/L). Reduction rates of O_2 and Fe were calculated as mg/m^2/day by multiplying by the volume of water above sediment (150 mL) and dividing by the surface area of sediment (0.0059 m^2). The surface area was calculated by multiplying the length of the bottle (9.8 cm) by the width of the bottle where the sediment reached (6 cm) and converted to m^2.

3.3 Results

3.3.1 O_2 Consumption

The rate of O_2 consumption was unaffected by NO_3^- concentration as all treatments reached O_2 concentration of less than 1 mg/L by the first sampling point at minimum rates of 9.3 ± 0.08 mg/m^2/day, 8.0 ± 0.76 mg/m^2/day and 9.4 ± 0.13 mg/m^2/day for the low, medium and high treatments respectively. After the initial decrease in O_2, concentrations remain at 0.5 mg/L. (Figure 3.2)

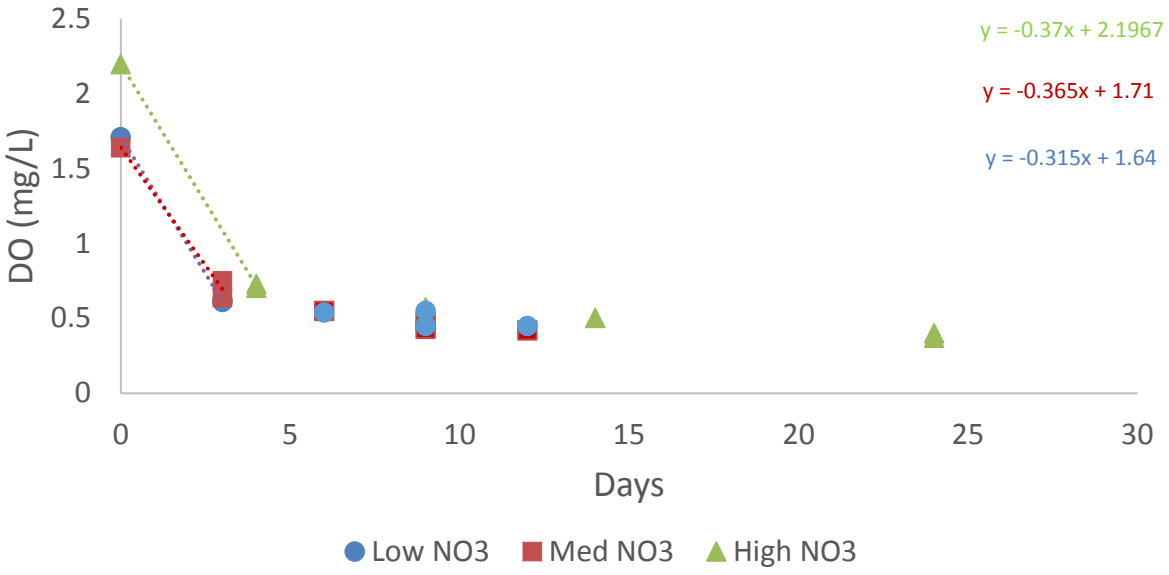

Figure 3.2: O_2 **concentration of the overlaying water during incubation plotted against time for the low (blue circle), med (red square) and high (green triangle)** NO_3^- **treatments. The rate of** O_2 **consumption for the low, med and high treatments were 8.1, 9.4 and 9.4** $mg/m^2/day$ **respectively.**

3.3.2 NO_3^- Consumption

Initial NO_3^- concentrations are 4-5% lower than the stock solutions for all treatments likely due to dilution with pore water. In addition, the detection limit of the method used to analyze NO_3^- concentrations is 0.05 mg-N/L with ± 0.02 mgN/L precision. In the low NO_3^- treatment consumption of NO_3^- follows a first order rate equation with a rate constant of 0.075 ± 0.04 $^{day\text{-}1}$. In the medium treatment NO_3^- consumption follows a rate constant of 0.095 ± 0.01 day^{-1} and in the high treatment NO_3^- consumption has a rate constant of 0.095 ± 0.02 day^- using first order decay fit.

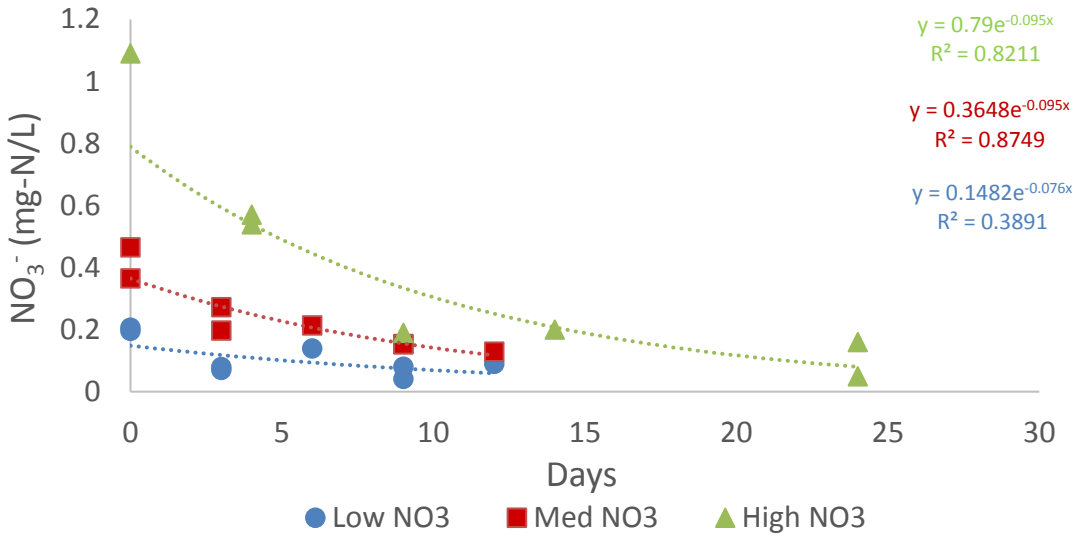

Figure 3.3: NO_3^- concentration of the overlaying water during incubation plotted against time for the low (blue circle), med (red square) and high (green triangle) NO_3^- treatments. First order rate equations fit the results with $R^2 > 0.8$ for both high and medium treatments while neither 0th or first order rates fit the low treatment well with $R^2 < 0.4$.

3.3.3 Fe Release

Initial TDFe concentrations of the stock solution used in the incubations were 0.03 mg/L. Upon addition of sediment to the solution (t=0 days), TDFe increased to 0.46, 0.13 and 0.34 mg/L for the low, medium and high NO_3^- treatments respectively. From t=0 the low NO_3^- incubation showed a constant Fe release of 12.8 ± 1.27 mg/m^2/day. While the medium and high NO_3^- incubations show Fe release during the early stages of their incubation, these increases are likely due to the sediment pore water (which likely had some amount of dissolved Fe already present) and overlaying water equilibrating with each other. In all three treatments the rate of Fe release observed after NO_3^- depletion was on average 70% faster than the rate of Fe release seen at the start which suggests that these two periods of release represent different processes. After 6 days, Fe release follows a linear rate of 12.5 ± 0.25 mg/m^2/day in the medium incubation which is similar to the rate seen in the low NO_3^- incubation. In the High NO_3^- incubation, release of Fe

is not seen until 14 days after the incubation began. After 14 days, Fe release follows a linear release rate of 10.9 mg/m^2/day (no uncertainty could reported as only two data points during Fe release were observed) were is similar to those seen in the low and medium NO_3^- incubations. A Dixon Q test, which determines if an outlying data point is statistically different, was conducted on the three rates of Fe release observed in the incubations. It was determined that the rate of 10.9 mg/m^2/day was not an outlier and as such is not significantly different than the other two rates. In all incubations Fe release was not observed until the concentration of NO_3^- reached 0.2 mg-N/L suggestion that there is a threshold value of NO_3^- concentration above which Fe release is prevented. By increasing the concentration of NO_3^- in the water overlaying anoxic sediment it is possible to delay the release of Fe from the sediment and, once Fe is released, it follows a similar linear rate regardless of the NO_3^- treatment applied.

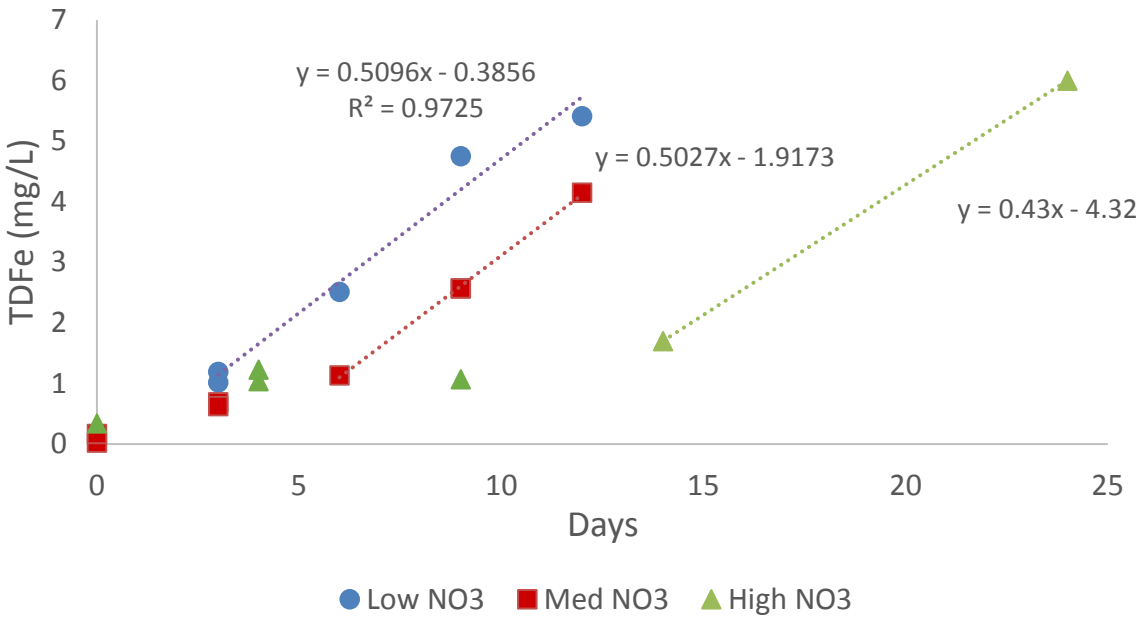

Figure 3.4: TDFe concentration of the overlaying water during incubation plotted against time for the low 0.21mg-N/L(blue circle), med 0.42mg-N/L (red square) and high 1.04mg-N/L(green triangle) NO_3^- treatments.

3.4 Discussion:

3.4.1 Role of NO_3^- in controlling Fe release from lake sediment

NO_3^- plays an integral role in controlling Fe release from hypolimnetic sediments in lakes that go anoxic during stratification by preventing Fe release across the sediment water interface either through oxidation of reduced Fe diffusing from deeper in the sediment, or, by preventing the reduction of Fe at the SWI. The difference between these two processes is large and results from this study suggest end results are indistinguishable from each other since only TDFe in the water column was measured. The oxidation of Fe(II) with NO_3^- is mediated by NO_3^--reducing bacteria that utilize NO_3^- as an electron acceptor and Fe(II) as an electron donor (Straub et al., 1996). The products of this process are N_2 gas and $Fe(OH)_3$. However, no measures were done to determine if this is the process that occurred. NO_3^- can also prevent the reduction of Fe(III) by acting as the main terminal electron donor for facultative anaerobes in the absence of oxygen. Following the redox ladder, once oxygen is depleted, NO_3^- will be preferentially reduced before Fe(III) (Straub et al., 1996). This is because the reduction of NO_3^- yields more energy than the reduction of Fe(III). However, once NO_3^- drops below approximately 0.2 mg-N/L, Fe release occurs at a constant rate which implies that, while initial NO_3^- concentration effects the timing of Fe release, it does not affect the rate of Fe release.

Similar results were found in a lake scale experiment in which NO_3^- was used to prevent the release of P from sediments in eutrophic, moderately hard watered White Lough (Foy,1986). White Lough has a surface area of 7.41 ha and a maximum depth of 10.7 m. The epilimnetic concentrations of SO_4^{2-} and NO_3^- are 22 mg/L and 0.74 mg/L, respectively. The first experiment applied a NO_3^- rich solution, 1m over the sediment, to assess the effectiveness of NO_3^- in reducing P loading from sediment in White Lough in North Ireland (Foy, 1986) (Figure 2.13). In

1982, the year without NO_3^- additions, Fe release occurred a month and a half earlier than in 1983, a year with NO_3^- additions. Once Fe release began in 1983 the rate of Fe release was similar to that seen in 1982.

A more recent study observing the potential use of NO_3^- in restoring water quality in Lake Lyng demonstrates the effect that continual additions of NO_3^- to the sediment has on Fe release compared to a single addition at the beginning of the stratification season (Søndergaard, 2000). Lake Lyng has a surface area of 10 ha and a maximum depth of 7.6 m. TP and NO_3^- concentrations during summer months average 0.61 mg-P/L and <0.01 mg-N/L, respectively. The concentration of Fe in the Hypolimnetic sediment was 33mg Fe/g When NO_3^- was continuously applied to sediment the release of Fe was substantially suppressed while NO_3^- was present. The year following the final addition of NO_3^- shows that Fe release proceeds unhindered once additions stopped and NO_3^- had been reduced (Figure 2.13). These studies suggests that the role that NO_3^- has on suppressing Fe release is short lived and that NO_3^- concentrations must be consistently high from year to year in order to prevent Fe release since NO_3^- is consumed relatively rapidly at the SWI in the absence of O_2.

3.4.2 Implication of NO_3^- control on Fe

The results from this chapter strongly suggest that reductions in spring NO_3^- concentrations (by decreasing N loading) cause Fe(II) to release from sediments earlier during stratification in the absence of O_2. In addition, internal P loading may be similarly affected since reduction of $Fe(OH)_3$ is thought to be closely linked to internal P release from the hypolimnion due to the binding affinity of P to $Fe(OH)_3$ (Amirbahman et al., 2003). As a result, low NO_3^- concentrations in the water column will lead to the ideal nutrient conditions hypothesized for

supporting N-fixing cyanobacteria growth (Low N, High P, High Fe(II)) occurring earlier in the summer, giving N-fixing cyanobacteria an advantage over other phytoplankton.

A wastewater treatment plant near Lake Tegel in Germany is an interesting case study due to the staggered implementation of NO_3^- removal. In 1992 the first stage, that of converting NH_4^+ to NO_3^-, was implemented which resulted in increased NO_3^- loading to Lake Tegel, which subsequently correlated to a decrease in peak TP concentrations from 0.5 mg/L to 0.2 mg/L in the lake. Once the second step, removing NO_3^- by denitrification to N_2, was implemented, TP concentrations returned to previously observed values (Schauser, 2006). The reduction in TP concentrations while NO_3^- loading was high was attributed to NO_3^- preventing the reduction of Fe oxides bound with P in the sediment (Beutel, 2016).

Occoquan Reservoir, a 6.2 km^2 reservoir located in Virginia, USA, is a case study where increased NO_3^- loads were intentionally used to improve water quality (Beutel, 2016). Water managers at Occoquan Reservoir discharge highly-treated waste water with low N concentrations the majority of the year. However, in the summer months, when the potential of anoxia at the bottom of the stratified reservoir is high, the treatment is altered to increase NO_3^- concentration. This NO_3^- rich water is released into the deepest part (19.8 m) of the reservoir. This has been shown to prevent the release of both TP and Fe, resulting in much lower TP concentrations during the summer (Cubas, 2014).

Both of these case studies agree with the results of the incubation which indicate that altering overlaying water column NO_3^- concentration can have a large impact on water quality including the accumulation of Fe(II) which is shown to promote cyanobacteria dominance of phytoplankton blooms (Verschoor et al., 2017). However, using the rate equation found for the reduction of NO_3^- in Sturgeon Bay, it was determined that, in order to maintain a concentration

of NO_3^- above 0.2 mg-N/L for 100 days, 34 tonnes of KNO_3^- would need to be added at the beginning of stratification. If instead KNO_3^- was added daily to keep NO_3^- concentrations at their initial level through the duration of stratification, it is necessary to add approximately 63 kg/day to the hypolimnion.

3.4.3 Controls on NO_3^- and Fe Rate Equations

In the absence of O_2, NO_3^- reduction rates are likely controlled by diffusion since rates observed, in both incubations and field work, follow first order kinetics. Diffusion of dissolved species is dependent on concentration gradients as well as the diffusion constant of the matrix they are dissolved in. High concentrations of a chemical species will diffuse to an area with a low concentration of that species. This rate becomes faster the greater the gradient in concentration. For NO_3^- this means that in early spring, NO_3^- is supplied quickly to the SWI interface where NO_3^- is present at low concentrations. This results in a high rate of NO_3^- reduction. As the NO_3^- in the water column becomes depleted the diffusion of NO_3^- to the SWI slows and the rate of NO_3^- reduction slows proportionately resulting in a first order rate equation.

Fe release rates appear to be linear suggesting that Fe release is not limited by diffusion. If Fe is not limited by diffusion there must be enough reducible Fe in the sediment to maintain a constant rate. It was shown in Chapter 2 that in the top two cm of sediment there is enough reducible Fe present that, at the rates observed in the field, Fe could release constantly for over 10 years. This means that the assumption that Fe release follows linear release rates is appropriate for the time scale that anoxia persists (approximately 100 days). This is important because, with a linear release rate, Fe accumulation will initially occur steadily in the absence of NO_3^-. If the Fe release rate was first order, Fe accumulation would proceed slowly at first and increase rapidly, promoting cyanobacteria growth suddenly. Although, a linear rate was

determined for Sturgeon Bay, L442 and L373 it is not expected that all lakes will show the same rate. Since Fe rates measured here are accumulation rates, it is possible that lakes that experience little physical mixing, due to factors such as storms, would have Fe accumulation rates that are first order since the stratification would prevent any mixing at the bottom of the hypolimnion.

3.4.4 Rates in Literature

Table 3.2 O_2, NO_3^- consumption rates and Fe release rates, observed in laboratory sediment core incubations, collected from literature.

Site	O_2 ($mg/m^2/day$)	NO_3^- (day^{-1})	NO_3^- ($mg/m^2/day$)	Fe ($mg/m^2/day$)	Source
Baldegg[a]	152	0.03			Mengis et al., 1997
Windemere[a]	15	0.04		20	Mortimer 1971
Sturgeon Bay	9	0.1		12.5	This Research
Gulf of Finland	275			6.3	Pakhomova et al., 2007
Lake Globsow	3.1				Wauer et al., 2004
San Vicente Reservoir[a]		0.74		0.01	Beutel. 2007
Lake 77 (Germany)[a]				140	Peine et al., 2000
Grahamstown[a]		0.13			Muller et al., 2015
Twitchell			30.0		Rudd et al., 1986
Big Moose			37.3		Rudd et al., 1986
Woods			23.3		Rudd et al., 1986
Sagamore			25.2		Rudd et al., 1986
Darts			34.5		Rudd et al., 1986

a = indicates where data was replotted in order to calculate rates; all other rates are as reported.

O_2 *Consumption rates*

In all three treatments, in the Sturgeon Bay sediment incubations conducted here, O_2 was consumed at an average rate of 9 $mg/m^2/day$. In Lake Windemere, a large (14.7 km^2) fresh water lake located in the United Kingdom with a depth of 60 m and Lake Baldegg, a 66 m deep eutrophic fresh water lake located in Switzerland, the O_2 consumption rate in sediment incubations are 15 $mg/m^2/day$ and 152 $mg/m^2/day$ respectively. In both of these incubations,

rates are higher than those observed during the incubation conducted on Sturgeon Bay sediment. Similarly, incubation experiments conducted using sediment collected from the Gulf of Finland, located on the eastern shore of the Black Sea, showed linear rates of O_2 consumption. However, the rate of O_2 consumption observed was 275 mg/m^2/day, over 30 times the rate observed during the Sturgeon Bay sediment incubations.

NO_3^- Consumption rates

In the case of NO_3^-, consumption rates in sediment core incubations were observed to follow both 0th and first order rate kinetics, depending on the study. A first order rate constant suggests that diffusion plays a large role on the availability of NO_3^- at the sediment water interface since at high NO_3^- concentrations the rate of reduction would be much greater. Rate constants range from 0.13 day^{-1} in Grahamstown Dam, a shallow (10m maximum depth) drinking water reservoir dominated by Sand and Siltstone geology, 20 km north of Newcastle Australia, to 0.028 day^{-1} in Lake Baldegg. The NO_3^- consumption rate constant for Sturgeon Bay sediment incubations lies toward the upper limit of the lakes listed here at 0.095 day^{-1}. Alternatively, Twitchell, Big Moose, Woods, Sagamore and Dart Lakes all follow 0th order rate equations. Rates in all of these lakes range from 30 mg/m^2/day to 37 mg/m^2/day implying that the concentration of NO_3^- does not affect the rate of NO_3^- reduction.

Fe Release Rates

Fe release rates from sediment in Sturgeon Bay and Windermere are similar at 12.5 mg/m^2/day and 20 mg/m^2/day, respectively. In Lake 77, a lake located within the Lausitz mining area in Germany, Fe release rates from sediment incubations reached 140 mg/m^2/day in the top cm of sediment, two orders of magnitude greater than the rates observed in Sturgeon Bay

sediments incubations. This is likely a result of the acidity (pH = 3) of the pore water observed in Lake 77. This is important because at low pH Fe becomes increasingly resistant to oxidation, in combination with the low O_2 concentrations during incubations, can result in a large flux of Fe from sediment.

In conclusion, O_2 reduction rates are similar in Sturgeon Bay, Windermere Lake and Lake Globsow ranging from 3.1 mg/m^2/day in Lake Globsow to 15 mg/m^2/day. Fe reduction rates range from 0.011 mg/m^2/day to 140 mg/m^2/day with Lake Windermere and the Gulf of Findland having similar rates to Sturgeon bay at 12.5 mg/m^2/day. NO_3^- reduction rate constants vary between lakes and in some cases are reported as a linear consumption rate.

3.4.5 Comparing Laboratory, Field and model Rates

Table 3.1. Reduction rates and rate constants for Sturgeon Bay, found in both field and incubation experiments, as well as, rates used to initialize the simple redox model developed in chapter 2.

	Sturgeon Bay					
	12m		10m		Sediment Incubation	Units
	Field	Model	Field	Model		
O_2	51	51	2020	2020	9	mg/m^2/day
NO_3^-	0.05	0.05	0.04	0.04	0.1	day^{-1}
Fe	61	94	1005	1270	12.5	mg/m^2/day
SO_4^{2-}	0.03	0.03	0.01	0.01	N/A	day^{-1}

Reduction rates for Fe and DO, measured in sediment incubation under laboratory conditions, are lower than those observed in field scale experiments (Table 3.1). However, the rate constant for the reduction of NO_3^- determined during the incubation experiment is higher than those observed in the field. The rates used in the model were rates that were measured in the field with the exception of Fe, where rates were increased to account for the fact that net

rates were measured in the field and that the model has a function that removes Fe from the system which would falsely decrease the end of summer concentrations.

3.5 Summary and Conclusion

Through sediment incubations with solutions of varying initial concentrations of NO_3^-, it was shown that the rate equations used in developing the parsimonious anoxic hypolimnetic Fe release model were appropriate. NO_3^- consumption rates changed with time, with the rate of change being identical in both the medium and high treatments suggesting that NO_3^- consumption follows a first order consumption rate. Fe release from sediments occurred when NO_3^- concentrations dropped below 0.2 mg-N/L in all treatments. Once Fe release began, it continued at similar linear rates at for all treatments suggesting that initial NO_3^- only delays the timing of Fe release and not the Fe release rate.

While research has been done on the ability of NO_3^- to delay and/or suppress the internal loading of P from sediments, most of this research largely focuses on concentrations of NO_3^- relative to P concentrations and just lightly covers the role that NO_3^- has on preventing the reduction of Fe. It is supported by the data presented here that, while observing the accumulation of P is important, studying the actual processes that result in P release is more important. In many sediments P is adsorbed to oxidized Fe and only releases into the water column upon the reduction and subsequent dissolution of Fe. The results in this chapter imply that higher initial concentration of NO_3^- in the water column above sediment in the anoxic zone of stratified lakes will result in Fe release being delayed later into the season. However, the initial concentration of NO_3^- has no effect on the rate at which Fe will release release once both the O_2 and NO_3^- are consumed.

This research focuses on the effect that NO_3^- has on the redox conditions at the SWI in the absence of O_2 in the hypolimnion of stratified lakes. If O_2 is always present at the SWI than no Fe reduction will occur and reduced and soluble Fe will remain low indefinitely, leaving cyanobacteria to rely on siderophores to scavenge Fe bound to dissolved organic carbon. However, the fact that NO_3^- controls redox in addition to being an important source of N for competitors to cyanobacteria, particularly to species that can fix atmospheric N_2, makes NO_3^- a significant factor to consider when studying the drivers of cyanobacteria dominance of phytoplankton blooms.

Chapter 4: Summary and Future Research

Phytoplankton blooms dominated by cyanobacteria, bacteria with the potential to produce hepato- and neurotoxins, are an ever increasing concern even in oligo-mesotrophic lakes. The cause of the increase in occurrence of these potentially harmful blooms is currently not well understood and there are currently few ways to predict the likelihood of a lake to support such a bloom. Using the two leading hypothesis regarding controls on cyanobacteria dominance (Fe(II) availability and N:P), as well as, basic redox equations for the reduction of four major redox species (NO_3^-, SO_4^{2-}, O_2 and Fe) a parsimonious model was constructed with the goal of predicting the time period that Fe(II) would become widely available in the hypolimnion of lakes in which the hypolimnion goes anoxic during stratification. In addition, the potential of altering NO_3^- concentrations at the SWI was assessed as a control of N-fixing cyanobacteria by increasing N:P ratios and limiting Fe release from anoxic sediments.

The model was then fit to field data collected from Sturgeon Bay and Deep Bay in 2015, as well as, historical data from L442 in 2006 and L373 in 2007. Rates of NO_3^-, O_2 and SO_4^{2-} consumption and Fe release were determined by observing the changes in concentrations of each redox species in the bottom 4m of the hypolimnion, divided into two 2 m strata, of these lakes over the summer stratification period (May-September). The model constructed using this method allowed the timing of Fe release in 2014 for Georgian Bay lakes, 2005 for L442 and 2006 for L373 to be predicted to within 10 days of when Fe release was observed in field samples in all Lakes at both intervals. Due to natural variability in rates and lake conditions, some deviation from field data was expected in the model. However, on average, the models show a good fit with a mean E of 0.73. It was also determined that rates observed in each 2 m interval of the lake are not consistent from one strata the next which means that modeling

multiple depths would require a full, season long, sampling profile to determine rates at these depths.

The effect that NO_3^- has on Fe release was determined to be one of buffering the redox conditions near the sediment water interface. In the experiment conducted, the incubation with high initial NO_3^- showed a Fe release after 14 days whereas the incubation with low initial NO_3^- showed Fe release immediately. However, it is important to note that the concentration of NO_3^- at the start of each incubation had no effect on the rate at which Fe accumulated after release commenced. What this research suggests is that, any potential efforts to reduce eutrophication of a lake, though the reduction of NO_3^- loading to the lake, may result in Fe release from sediment occurring earlier during stratification in anoxic hypolimnions and promote cyanobacteria growth. A better method would be to reduce NO_3^- loading during winter season where it would build up in lakes and increase the NO_3^- loading during the spring, directly to the hypolimnion, where it will be consumed in the absence of O_2 preventing the accumulation of Fe. High concentrations of NO_3^- could be added to the hypolimnion of lakes such as Sturgeon Bay since NO_3^- is rapidly consumed and should not allow surfacewater NO_3^- concentrations to exceed 10 mg/L. This research shows that Fe, in the lakes studied, is redox sensitive and that increasing the redox potential at the SWI is a potential management tool.

Further Research

While the model constructed here preforms well in predicting the timing of Fe release (E= 0.73), the model does not completely capture how Fe concentrations change after release has begun. One hypothesis on why this may be is that here, water column SO_4^{2-} concentrations were used to model sulfide formation and subsequent Fe-S precipitation, however, it may be that

measuring early summer SO_4^{2-} pore water concentrations and using those to model Fe-S precipitation may be more accurate. This is because SO_4^{2-} reduction occurs below the sediments surface away from all other electron acceptors. As a result, sulfide could form deeper in the sediment, causing diffusion of sulfide up towards the SWI. Since Fe is utilized as an electron acceptor before SO_4^{2-}, Fe reduction would still occur at the SWI but the rate of release into the water column would be hindered by the formation of Fe-S compounds formed when sulfide diffuses up from deeper in the sediment. I propose that utilizing pore water SO_4^{2-} concentrations would help determine why in some sites Fe release appears to be non-linear when my own research as well as in literature find that the rate of Fe release appears to be constant.

A much more ambitious project would be to assess how a lake that is known to experience regular cyanobacterial blooms, reacts to the addition of NO_3^- in to the hypolimnion at different periods in stratification. While this would be a long, multi-year experiment it would be interesting to see how adding NO_3^- prior to stratification, prior to predicted timing of Fe release, and after Fe release begins effects both Fe release timing as well as cyanobacteria dominance. In addition, the type of sediment in these lakes could be analyzed to determine their Fe:P ratio in order to build a data base of lakes that are likely to experience cyanobacteria blooms due to lowered NO_3^- loads.

In conclusion, a parsimonious model based on the reduction of NO_3^-, O_2, SO_4^{2-} and Fe can predict how many days after initial sampling Fe release is expected to occur to within 10 days and that such a model can be fit using rates calculated from field samples collected every 2 weeks from May-September during a single year from the hypolimnion. The model then only needs a single sampling trip in May of subsequent years in order to be run. It was also shown that the presence of NO_3^-, at concentrations of <0.2 mg-N/L effectively prevents Fe reduction at the

SWI and delays the release of soluble Fe to the water column. This suggests that NO_3^- loading to the hypolimnion of lakes that go anoxic during stratification and experience cyanobacteria dominated blooms should be seriously considered as a potential management practice in the prevention of cyanobacteria growth.

References

Beutel, M.W., Horne, A.J., Taylor, H.W.D., Losee, R.F., Whitney, R.D. 2009. Effects of oxygen and nitrate on nutrient release from profundal sediments of a large, oligo-mesotrophic reservoir, Lake Mathews, California. Lake and Reservoir Management. 24: pp. 18-29.

Beutel, M.W., et al., 2016. A review of managed nitrate addition to enhance surface water quality. Environmental Science and Technology. Vol 46, NO.7 pp 673-700

Brimblecomb, P., Clegg, S.L., Davies, T.D., Shooter, D., Tranter, M. 1987. Obersvations of the preferential loss of major ions from melting snow and laboratory ice. Wat. Res. 21: pp 1279-1286.

Bouffard, D., Ackerman, J.D., Boegman, L. 2013. Factors affecting the development and dynamics of hypoxia in a large shallow stratified lake: hourly to seasonal patterns. Water Resources Research. Vol. 49. pp 2380-2394.

Brunskill, G.J., and Schindler, D.W. 1971. Geography and bathymetry of selected lake basins, Experimental Lakes Area, northwestern Ontario. J. Fish. Res. Bd. Canada 28:139-155.

Canfield, D.E., Thamdrup, B., Hansen, J.W. 1933. The anaerobic degradation of organic matter in Danish Coastal sediments: Iron reduction, manganese reduction, and sulfate reduction. Geochimica et Cosmochimica acta. 57: pp. 3867-3883.

Cubas, F., Novak, J.T., Godrej, A.N., Grizzard, T.J. 2014. Effects of Nitrate Input from a Water Reclamation Facility on the Occaquan Reservoir Water Quality. Water Environment Research, Volume 86, Number 2, pp. 123-133.

Culshaw, N.G., Corrigan, D., Ketchum, J.W.F., Wallace, P. and Wodicka, N. 2004. Precambrian geology, Naiscoot area; Ontario Geological Survey, Preliminary Map P.3549

Daloğlu, I., Cho, K., Scavia, B., 2012. Evaluating causes of trends in long-term dissolved reactive phosphorus loads to Lake Erie. Environmental Science & Technology, 46, 10660-10666.

Davidson, W., Heaney, S.I., Talling, J.F., Rigg, E. 1980. Seasonal transformations and movements of iron in productive English lake with deep-water anoxia. Schwizerische Zeitschrift für Hydrologie. Vol 42, issue 2, pp 196-224

De Stasio, Jr., Hill, D.K., Kleinhans, J.M., Nibbelink, N.P., and Magnuson, J.J. 1993. Potential effects of global climate change on small north-temperate lakes: Physics, fish, and plankton 41 1136-1149

Deep Bay association. 2012. Deep Bay Watershed & Lake Management plan. 4.1: pp.28-31.

Downing, J.A., Watson, S.B., McCauley, E. 2001. Predicting Cyanobacteria Dominance in Lakes. Canadian Journal of Fisheries and Aquatic Sciences. 58: pp. 1905-1908.

Engle T., Reid P. 2006. Thermodynamics, Statistical Thermodynamics, & Kinetics. Upper Saddle River, NJ: Pearson Education.

Farrar K., Bryant D., Cope-Selby N. 2014. Understand and engineering beneficial plant-microbe interactions: plant growth promotion in energy crops. Plant Biotechnology Journal. 12: pp 1193-1206.

Fitzsimmons, E. (2014, August 4). Tap Water Bans for Toledo Residents. The New York Times. pg. A12. Retrieved from (https://www.nytimes.com/2014/08/04/us/toledo-faces-second day^{-1}of-water-ban.html)

Foy, R.H. 1986. Suppression of Phosphorus Release From Lake Sediments by the Addition of Nitrate. Wat. Res. Vol. 20 pp. 1345-1351.

Frey, B.C., Mutz, A. 2007. The Public Trust in Surface Waterways and Submerged Lands of The Great Lakes States. University of Michigan Journal of Law Reform. Vol. 40:4. pp. 908-993.

Galloway et al., 2008. Transformation of the Nitrogen Cycle: Recent Trends, Questions, and Potential Solutions. Science. Vol. 320. pp 889-892.

Glass, JB., Wolfe-Simon FW, Anbar AD. 2009. Coevolution of metal availability and nitrogen assimilation in cyanobacteria and metal. Geobiology. 7: pp.100–123.

Glud, R.N., Berg, P., Fossing, H., Jørgensen, B.B. 2007. Effect of the diffusive boundary layer on the benthic mineralization and O_2 distribution: A theoretical model analysis. Limnology and Oceanography 52: pp. 547-557.

Guildford, S.J., Hecky, R.E. 2000. Total Nitrogen, Total Phosphorus, and Nutrient Limitation in Lakes and Oceans: Is There a Common Relationship? Limnology and Oceanography. Vol 45. pp 1213-1223.

Haghseresht, F., Wang, S., Do, D.D. 2009. A novel lanthanum-modified bentonite, Phoslock, for phosphate removal from wastewaters. Applied Clay Science. 46: issue 4 pp. 69-375

Hall, P.O.J., Anderson, L.G., Rutgers van der Loeff, M.M., Sundby, B. and Westerlund, S.F.G.,1989. Oxygen uptake kinetics in the benthic boundary layer. Limnology and Oceanogrraphy. 34: pp. 734-746.

Havens, K.E. 2008. Cyanobacteria blooms: effects on aquatic ecosystems. Advances in Experimental Medicine and Biology. Vol. 619. pp 733-747.

Head, R.M., Jones, R.I., Bailey-Watts, A.E. 1999. Vertical movements by planktonic cyanobacteria and the translocation of phosphorus: implications for lake restoration. Aquat Conserv. 9: pp 111–120.

Hecky, R.E., Kilham, P. 1998. Nutrient limitation of phytoplankton in freshwater and marine environments: A review of recent evidence on the effects of enrichment. Limnol. Oceanogr. 33(4), pp 796-822.

Jetoo, S., Grover, V.I., Krantzberg, G. 2015. The Toledo Drinking Water Advisory: Suggested Application of the Water Safety Planning Approach. Sustainability. 7(8): pp 9787-9808.

Kalff, J. 2002. Limnology. Upper Saddle, NJ. Prentice-Hall.

Knowles, R. 1982. Denitrification. Microbiological Reviews. 46: pp43-70

Loh et al., 2013. Evaluating relationships between sediment chemistry and anoxic phosphorus and iron release across three different water bodies. Inland Waters. 3: pp.105-118

Mengis, M., Gächter, R., Wehrli, B. 1997. Nitrogen elimination in two deep eutrophic lakes. Limnology and Oceanography. 42: pp. 1530-1543.

Meyers, P.A., Ishiwatari, R 1993. Lacustrine organic geochemistry- an overview of indicators of organic matter sources and diagenesis in lake sediments. Org. Geochem. Vol. 20: pp.867-900

Miller, M.J. et al., 1986. Quaterneary Geoilogy of the Parry Sound Area, District of Parry Sound; Ontario Geological Survey. Map P.3102.

Ministry of Agriculture, Food and Rural Affairs. 2002. Nutrient Management Act. O. Reg. 267/03.

Molot L.A., Dillon P.J. 1993. Nitrogen mass balances and denitrification rates in central Ontario Lakes. Biogeochemistry. 20: pp. 195-212

Molot L.A., Li G., Findlay D.L. & Watson S.B. (2010) Iron mediated suppression of bloom forming cyanobacteria by oxine in a eutrophic lake. Freshwater Biology. 55: pp. 1102 1117.

Molot et al., 2014. A novel model for cyanobacteria bloom formation: the critical role of anoxia and ferrous iron. Freshwater Biology.

Morel, F.M.M. & Hering, J.G. 1993. Principles and Applications of Aquatic Chemistry. JohnWiley and Sons Inc., Toronto.

Mortimer, C. H. 1941. The exchange of dissolved substances between mud and water in lakes. Journal of Ecology 29: pp. 280–329.

Mortimer, C.H. 1971. Chemical Exchanges Between Sediments and Water in the Great Lakes Speculations on Probable Regulatory Mechanisms. Limnology and Oceanography. 16: pp.387 – 404.

Mostofa, K., Yoskioka, T., Mottaleb, M. & Vione, D. 2013. Photobiogeochemistry of Organic Matter: Principles and Practices in Water Environments. Springer, Berlin, Heidelberg.

Murray, T.E. 1995. The correlation between iron sulfide precipitation and hypolimnetic phosphorus accumulation during one summer in a softwater lake Canadian Journal of Fisheries and Aquatic Sciences, 52(6): 1190-1194, 10.1139/f95-115

Müller, S., Mitrovic, S.M., Baldwin, D.S. 2016. Oxygen and dissolved organic carbon control release of N,O and Fe from the sediment of a shallow, polymictic lake. Journal of Soils and Sediments. 16: pp. 1109-1120.

Nürnberg, G.K., 2009. Assessing internal phosphorus load – problems to be solved. Lake Reserv Manage. 25: pp.419-32.

Orihel, D. 2013. The role of iron in suppressing internal phosphorus loading and toxic cyanobacterial blooms in freshwater lakes. University of Alberta. Department of Biological Sciences.

Pace, M..L, Prairie, Y.T. 2005. Respiration in lakes. In: del Giorgio PA, Williams PJ leB, Eds. Respiration in Aquatic systems. Oxford: Oxford University Press. pp 103–121

Pakhomova, S.V., Hall, P.O.J., Kononets, M.Y., Rozanov, A.G., Tengber, A., Vershinin, A.V. 2007. Fluxes of iron and manganese across the sediment-water interface under various redox conditions. Marine Chemistry. 107: pp. 319-331.

Peine, A., Tristschler, A., Küsel, K., Peiffer, S. 2000. Electron flow in an iron-rich acidic sediment- evidence for an acidity-driven iron cycle. Limnology and Oceanography. 1077-1087.

Rich, P,H. 1980. Hypolimnetic Metabolism in Three Cape cod Lakes. The American Midland Naturalist. 104: pp. 102-109.

Roach, John. 2007. Source of Half Earth's Oxygen Gets Little Credit. National Geographic.

Roden, E. & J. Edmonds. 1997. Phosphate mobilization in iron-rich anaerobic sediments: microbial Fe(III) oxide reduction versus iron-sulfide formation. Arch. Hydrobiol. 139: 347-378

Rudd, J.W.M., Kelly, C.A., St. Louis, V., Hesslein, R.H., Furutani, A., Holoka, M.H. 1986. Microbial Consumption of nitric and sulfuric acids in acidified north temperate lakes. Limnology and Oceanography. 31: 1726-1280.

Ruttenberg, K.C. 2003. The Global Phosphorus Cycle. Treatise on Geochemistry. 8: pp. 585-643

Santschi, P., Höhener, P., Benoit, G., Brink. M.B. 1990. Chemical processes at the sediment water interface. Marine Chemistry. 30: pp. 269-315.

Scavia, D., et al., 20014. Assessing and Addressing the Re-eutrophication of Lake Erie: Central basin hypoxia. Journal of Great Lakes Research. 40: pp. 226-246.

Schauser, I., Chorus, I., Lewandowski J. 2006. Effects of nitrate on phosphorus release: comparisons of two Berlin lakes. Acta hydrochim. hydrobiol. 2006, 34, 325 – 332.

Schiefer, K. 2003. Water Quality Study of Sturgeon Bay. A Report Prepared for the Township of the Archipelago. December 2003.

Schindler, D.W. & Curtis, P.J. 1997. The role of DOC in protecting freshwaters subjected to climatic warming and acidification from UV exposure. Biogeochemistry 36: 1-8.

Sinsabaugh, R.L., & Findlay, S. (2003) Dissolved Organic Matter: Out of the Black Box into the Mainstream. In "Aquatic Ecosystems: Interactivity of Dissolved Organic Matter" Eds S.E.G. Findlay and R.L. Sinsabaugh, pp 479- 498. Academic Press, New York.

Smil V. 2000. Phosphorous in the Environment: Natural Flows and Human Interferences. Annual Review of Energy and the Environment. 25: pp. 53-88.

Smith, V.H. 1983. Low Nitrogen to Phosphorous Ratios Favor Dominance by Blue-Green Algae in Lake Phytoplankton. Science. 221: pp. 669-671.

Smith, V.H., G.D. Tilman, J.C. Nekola. 1999. Eutrophication: impacts of excess nutrient inputs on freshwater, marine, and terrestrial ecosystems. Environmental Pollution. 100: pp. 179 196.

Søndergaard, M., Jeppesen, E. & Jensen, J.P. 2000. Hypolimnetic Nitrate Treatment to Reduce Internal Phosphorus Loading in a Stratified Lake, Lake and Reservoir Management, 16:3, 195-204, DOI: 10.1080/07438140009353963

Sorichetti, R.J. 2013. Iron-Regulated Cyanobacterial Predominance and Siderophore Production in Oligotrophic Freshwater Lakes. University of Western Ontario Electronic Thesis a Dissertation Repository.

Straub, K.L., Benz, M., Schink, B., Widdel., F. 1996. Anaerobic, Nitrate-Dependent Microbial Oxidation of Ferrous Iron. Applied and Environmental Microbiology. pp. 1458-1460

Stumpf, R.P., Wynne, T.T, Baker, D.B., Fahnensiel, G.L. 2012. Interannual Variability Of Cyanobacterial Blooms in Lake Erie. PLoS ONE 7(8): e42444.

Sundby, B., Anderso, L.G., Hall, P.O.J., Jverfeldt, A., Rutgers Van Der Loeff, M.M., Westerlund, S.F.G. 1986. The effect of oxygen on release and uptake of cobalt, manganese, iron and phosphate at the sediment-water interface. Geochimica et Cosmochimica acta 50: pp. 1281-1288.

Thramdrup, B. 2012. New Pathways and Processes in the Global Nitrogen Cycle. Annual Review of Ecology, Evolution and Systematics. 43: pp. 407-428.

Verschoor, M. et al., 2017. Internal iron loading and warm temperatures are a pre-condition for cyanobacterial dominance in embayments along Georgian Bay, Great Lakes. Canadian Journal of Fisheries and Aquatic Sciences. 0, 0, 10.1139/cjfas-2016-0377.

Wetzel, R.G. 2001. Limnology: Lake and River Ecosystems 3rd Edition. Academic Press: San Diego.

Wilhelm S. 1995. Ecology of iron-limited cyanobacteria: a review of physiological responses and implications for aquatic systems. Aquat Microbial Ecol. 9: pp. 295–303.

Wilhelm S. & Trick C.G. (1994) Iron-limited growth of cyanobacteria-multiple siderophores production is a common response. Limnology and Oceanography. 39: pp. 1979-1984.

Winter, J.G. et al., 2011. Alagal blooms in Ontario, Canada: Increases in reports since 1994. Lake reservoir management. 27: pp. 107-114.

Appendix

Table 5.1. Full chemical profiles collected from Sturgeon Bay and Deep Bay from the summer of 2014 and 2015

Sturgeon Bay 2014						
Sample ID	Depth (m)	Temperature (^oC)	DO (mg/L)	SO_4^{2-} (mg/L)	NO_3^- (mgN/L)	Fe (mg/L)
SBJN16-0/3	1.5	20.7	8.8			0.1
SBJN16-4/7	5.5	17.6	6.4			0.1
SBJN16-8	8	11.5	4.8			0.1
SBJN16-10	10	9.9	2.1			0.1
SBJY08-0/4	2	21.8	8.6	4.9	0.2	0.1
SBJY08-5/9	7	15.4	1.1	4.8	0.3	0.2
SBJY08-10	10	10.0	0.3	4.6	0.2	0.4
SBJY08-12	12	9.8	0.2	4.4	0.2	0.9
SBJY28-0/5	2.5	21.4	7.4	5.2	0.1	0.1
SBJY28-6/9	7.5	18.4	0.5	4.8	0.1	0.3
SBJY28-8	8	14.6	0.3			0.3
SBJY28-10	10	11.0	0.2	4.2	<dl	1.4
SBJY28-12	12	10.1	0.2	3.7	0.1	2.5
SBAG25-0/7	3.5	22.1	9.2	5.3	0.1	0.1
SBAG25-8/9	8.5	18.2	3.6	6.3	0.1	0.1
SBAG25-10	10	10.7	0.3	3.2	0.2	3.1
SBAG25-12	12	10.3	0.2	1.2	0.1	4.9
SBSE16-0/8	4	16.9	8.5	5.8	0.1	0.1
SBSE16-9/10	9.5	16.2	6.6	5.8	0.1	0.2
SBSE16-11	11	11.9	0.4	5.0	0.1	0.5
SBSE16-13	13			5.0	0.2	7.9

Sturgeon Bay 2015

Sample ID	Depth (m)	Temperature (^oC)	DO (mg/L)	SO_4^{2-} (mg/L)	NO_3^- (mg/L)	Fe (mg/L)
SB June 15 epi	3	20.1	8.2	3.7	0.3	0.2
SB June 15 meta	8	19.3	5.2	3.6	0.3	0.2
SB June 15 10 m	10	8.1	3.2	3.5	0.5	0.2
SB June 15 12 m	12	7.1	2.0	3.5	0.8	0.3
SB June 29 Epi	2	21.1	8.6	3.9	0.6	0.1
SB June 29 Meta	8	15.0	3.3	3.7	0.3	0.2
SB June 29 12 m	12	7.6	0.7	3.5	0.4	0.3
SB July 13 epi	1.5	24.5	9.0	4.2	0.6	0.1
SB July 13 meta	6	19.5	3.9	4.0	0.6	0.1
SB July 13 9 m	9	14.6	0.7	3.7	0.7	0.2
SB July 13 11 m	11	10.2	0.1	3.5	0.4	0.3
SB July 13 13 m	13	8.4	0.1	3.7	0.3	1.1
SB July 27 0-6 m	3	22.9	7.0	4.6	0.6	0.1
SB July 27 7-8 m	7.5	17.7	3.2	4.3	0.6	0.2
SB July 27 9 m	9	12.3	0.2	3.7	0.1	0.6
SB July 27 11 m	11	9.1	0.1	3.3	0.1	1.2
SB July 27 13 m	13	8.3	0.1	3.0	0.1	2.9
SB Aug 10 0-7 m	3.5	22.0	7.1	4.9	0.6	0.2
SB Aug 8-9 m	8.5	17.6	3.1	4.4	0.6	0.2
SB Aug 10 10 m	10	10.2	0.2	3.1	0.3	1.9
SB Aug 10 12 m	12	8.9	0.1	2.0	0.5	3.5
SB Sep 1 0-9 m	4.5	20.8	7.4	5.9	0.1	0.1
SB Sep 1 10-11 m	10.5	14.9	0.2	2.9	0.4	3.1
SB Sep 1 12 m	12	9.9	0.1	0.9	0.3	5.9
SB Sep 14 0-9 m	4.5	20.0	7.9	6.1	0.4	0.1
SB Sep 14 10-11 m	10.5	15.5	1.7	3.3	0.4	2.6
SB Sep 14 12 m	12	10.7	0.7	0.5	0.5	6.5
SB Sep 28 0-10 m	5	19.0	8.1	7.0	0.7	0.1
SB Sep 28 11 m	11	15.5	0.3	4.7	0.7	0.8
SB Sep 28 12 m	12	11.2	0.2	0.9	0.5	7.7

Sturgeon Bay 2015

Sample ID	DOC (mgC/L)	DIC (mgC/L)	□13C-DIC	TDN (mg/L)	NO_2^- (mg/L)	NH_4^+ (mg/L)
SB June 15 epi	5.50		-6.02	0.40	<dl	<dl
SB June 15 meta	7.80		-11.06	0.40	<dl	<dl
SB June 15 10 m	6.40		-14.90	0.40	<dl	<dl
SB June 15 12 m	6.30		-16.55	0.40	0.17	<dl
SB June 29 Epi		5.94			0.04	<dl
SB June 29 Meta		7.81			0.00	<dl
SB June 29 12 m		10.69			0.00	0.10
SB July 13 epi	7.82	6.68	-4.46	0.07	<dl	<dl
SB July 13 meta	6.52	8.14	-11.37	0.18	<dl	<dl
SB July 13 9 m	6.25	9.71		0.14	0.01	<dl
SB July 13 11 m	6.65	10.47	-16.82	0.26	<dl	<dl
SB July 13 13 m	7.16	11.88	-18.83	0.23	0.03	0.08
SB July 27 0-6 m	7.78	8.05		0.16	<dl	<dl
SB July 27 7-8 m	7.90	9.19		0.26	<dl	<dl
SB July 27 9 m	6.37	10.92		0.23	<dl	<dl
SB July 27 11 m	6.53	11.36		0.14	<dl	0.13
SB July 27 13 m	7.74	12.52		0.36	<dl	<dl
SB Aug 10 0-7 m	5.90	7.83			<dl	<dl
SB Aug 8-9 m	6.93	9.29			<dl	<dl
SB Aug 10 10 m	8.27	11.14			<dl	0.08
SB Aug 10 12 m	9.04	12.39			<dl	0.23
SB Sep 1 0-9 m	5.65	8.03			<dl	<dl
SB Sep 1 10-11 m	8.39	11.07			<dl	<dl
SB Sep 1 12 m	9.52	12.32			<dl	0.15
SB Sep 14 0-9 m		9.25			<dl	<dl
SB Sep 14 10-11 m		12.16			<dl	0.12
SB Sep 14 12 m		15.02			<dl	<dl
SB Sep 28 0-10 m					<dl	<dl
SB Sep 28 11 m					<dl	<dl
SB Sep 28 12 m					<dl	<dl

Deep Bay 2014

Sample ID	Depth (m)	Temperature (°C)	DO (mg/L)	SO_4^{2-} (mg/L)	NO_3^- (mg/L)	Fe (mg/L)
DBJN17-0/3	1.5	20.2	9.3			0.1
DBJN17-4/6	5	14.3	7.2			0.1
DBJN17-7	7	10.6	6.5			0.1
DBJN17-9	9	8.9	5.9			0.1
DBJN17-11	11	7.2	5.6			0.1
DBJN17-13	13	6.5	5.1			0.1
DBJN17-15	15	6.4	4.7			0.2
DBJY09-0/3	1.5	20.6	8.4	5.7	<dl	0.1
DBJY09-4/5	4.5	18.5	6.2	5.6	0.1	0.1
DBJY09-6	6	12.3	3.9	5.3	0.3	0.1
DBJY09-10	10	8.3	3.1	5.3	0.3	0.2
DBJY09-12	12	7.0	2.9	5.2	0.1	0.2
DBJY09-14	14	6.6	2.3	5.1	0.2	0.2
DBJY09-16	16	6.4	1.8	5.1	0.2	0.2
DBJY28-0/5	2.5	22.0	7.8	5.6	0.1	0.1
DBJY28-6/8	7	12.9	1.6	5.4	0.2	0.2
DBJY28-9	9	9.6	1.4	5.2	0.2	0.2
DBJY28-11	11	7.7	1.7	5.1	0.2	0.2
DBJY28-13	13	6.7	1.1	5.1	0.3	0.2
DBJY28-15	15	6.6	0.7	5.0	0.1	0.2
DBJY28-17	17	6.5	0.3	4.9	0.1	0.3
DBAG25-0/4	2	22.3	9.7	11.7	0.1	0.1
DBAG25-5/10	7.5	14.1	0.3	5.3	0.1	0.3
DBAG25-11	11	8.1	0.2	4.8	0.1	0.5
DBAG25-13	13	6.9	0.2	4.9	0.1	0.5
DBAG25-15	15	6.7	0.2	6.2	0.4	0.7
DBAG25-17	17	6.7	0.2			0.7
DBSE17-0/5	2.5			6.2	0.2	0.1
DBSE17-6/9	8			6.3	0.1	0.1
DBSE17-10	10			6.4	0.1	0.1
DBSE17-12	12			5.3	0.2	0.3
DBSE17-14	14			4.4	0.1	1.9
DBSE17-17	17			4.1	0.1	4.4

Deep Bay 2015

Sample ID	Depth (m)	Temperature (°C)	DO (mg/L)	SO_4^{2-} (mg/L)	NO_3^- (mg/L)	Fe (mg/L)
DB June 16 epi	1	19.1	9.2	4.7	0.5	0.1
DB June 16 meta	4.5	13.8	7.7	4.8	0.3	0.1
DB June 16 7m	7	10.5	6.5	4.7	0.8	0.2
DB June 16 9m	9	9.1	5.9	4.7	0.9	0.2
DB June 16 11m	11	7.9	5.5	4.8	1.0	0.2
DB June 16 13m	13	6.7	4.5	4.7	0.7	0.2
DB June 16 15m	15	6.6	4.0	4.5	0.9	0.2
DB June 16 19m	19	6.4	3.5	4.4	0.6	0.3
DB June 29 epi	1.5	19.9	8.3	4.9	0.2	0.1
DB June 29 Meta	4.5	17.5	7.3	5.0	0.6	0.1
DB June 29 6	6	12.5	5.2	4.8	0.9	0.1
DB June 29 8	8	10.7	4.5	4.5	0.6	0.2
DB June 29 10	10	8.6	4.2	4.7	0.8	0.2
DB June 29 12	12	8.6	3.9	4.8	1.4	0.2
DB June 29 14	14	6.8	3.2	4.6	1.4	0.2
DB June 29 16	16	6.6	2.7	4.5	1.3	0.3
DB June 29 18	18	6.6	2.4	4.5	0.8	0.4
DB July 13 epi	1.5	23.8	9.2	5.0	0.4	0.1
DB July 13 meta	5.5	17.3	4.8	5.1	0.7	0.1
DB July 13 8m	8	11.9	2.8	4.7	0.9	0.2
DB July 13 10m	10	9.4	2.5	4.7	1.1	0.2
DB July 13 12m	12	8.0	2.4	4.7	1.2	0.2
DB July 13 14m	14	7.2	1.5	4.6	1.6	0.3
DB July 13 16m	16	7.0	0.8	4.4	1.6	0.5
DB July 27 0-4 m	2	23.2	8.3	5.3	0.6	0.1
DB July 27 5-11m	8	11.8	2.6	4.8	1.1	0.2
DB July 27 12 m	12	7.5	1.4	4.6	1.4	0.3
DB July 27 14 m	14	6.8	0.8	4.5	1.6	0.4
DB July 27 16 m	16	6.7	0.2	4.4	1.7	0.5
DB July 27 18 m	18	6.7	0.0	4.3	1.5	0.7
DB July 27 20 m	20	6.7	0.0	4.3	1.5	0.9
DB Aug 10 0-3 m	1.5	22.3	7.8	5.5	0.6	0.1
DB Aug 10 4-11 m	7.5	15.0	2.5	5.0	1.0	0.2
DB Aug 10 12 m	12	7.6	0.2	4.5	1.5	0.4
DB Aug 10 14 m	14	7.0	0.1	4.3	1.3	0.7
DB Aug 10 16 m	16	6.8	0.1	4.2	1.2	0.9
DB Aug 10 18 m	18	6.8	0.1	4.1	1.0	1.3

Sample ID	Depth (m)	Temperature (^{o}C)	DO (mg/L)	SO_4^{2-} (mg/L)	NO_3^- (mg/L)	Fe (mg/L)
DB Aug 10 20 m	20	6.8	0.1	3.9	0.8	2.7
DB Sep 1 0-5 m	2.5	20.8	7.5	6.2	0.4	0.1
DB Sep 1 6-13 m	9.5	12.4	1.1	4.8	0.6	1.0
DB Sep 1 14 m	14	7.3	0.1	6.7	0.6	1.6
DB Sep 1 16 m	16	7.0	0.2	4.3	0.6	2.4
DB Sep 1 18m	18	6.9	0.1	3.9	0.6	4.8
DB Sep 1 20m	20	6.9	0.1	3.7	0.4	5.9
DB Sep 14 0-6 m	3	19.9	7.4	6.1	0.7	0.1
DB Sep 14 7-11 m	9	14.5	1.4	4.7	0.7	1.2
DB Sep 14 12 m	12	8.9	0.2	4.2	0.7	2.0
DB Sep 14 14 m	14	7.6	0.2	4.0	0.7	3.1
DB Sep 14 16 m	16	7.2	0.1	5.6	0.7	4.8
DB Sep 14 18 m	18	7.0	0.2	4.0	0.7	5.8
DB Sep 14 20 m	20	7.0	0.2	4.1	0.4	6.3
DB Sep 28 0-8m	4	19.1	7.9	6.4	0.8	0.1
DB Sep 28 9-12 m	10.5	12.9	0.6	4.5	0.7	1.9
DB Sep 28 13m	13	8.4	0.2	4.2	0.7	5.2
DB Sep 28 15 m	14	7.4	0.2	3.7	0.7	6.3
DB Sep 28 17 m	15	7.1	0.2	3.3	0.7	4.0

Deep Bay 2015

Sample ID	DOC (mgC/L)	DIC (mgC/L)	13C-DIC	TDN (mg/L)	NO_2^- (mg/L)	NH_4^+ (mg/L)
DB June 16 epi	5.5		-2.9	0.4	<dl	<dl
DB June 16 meta	6.9		-5.8	0.4	<dl	0.16
DB June 16 7m	5.8		-10.8	0.3	<dl	<dl
DB June 16 9m	5.8		-11.9	0.4	<dl	<dl
DB June 16 11m	4.5		-13.4	0.2	<dl	<dl
DB June 16 13m	5.2		-14.9	0.3	<dl	<dl
DB June 16 15m	6.8		-15.7	0.3	<dl	0.15
DB June 16 19m	5.6		-17.5	0.4	0.13	<dl
DB June 29 epi		6.7	-3.3		<dl	<dl
DB June 29 Meta		7.5	-9.4		<dl	<dl
DB June 29 6		8.2	-14.6		<dl	<dl
DB June 29 8		8.8	-15.9		<dl	<dl
DB June 29 10		9.3	-16.7		<dl	<dl
DB June 29 12		9.6	-18.1		<dl	<dl
DB June 29 14		9.8	-18.8		<dl	<dl
DB June 29 16		10.1			<dl	<dl
DB June 29 18		10.8			<dl	0.05
DB July 13 epi	8.0	6.7		0.3	<dl	<dl
DB July 13 meta	5.7	8.1		0.3	<dl	<dl
DB July 13 8m	6.6	9.1		0.3	<dl	<dl
DB July 13 10m	7.4	9.4		0.4	<dl	<dl
DB July 13 12m	6.1	9.8		0.3	<dl	<dl
DB July 13 14m	7.1	10.5	1.5	0.5	<dl	<dl
DB July 13 16m	5.9	10.7	0.8	0.4	<dl	<dl
DB July 27 0-4 m	6.9	7.3	8.3	0.2	<dl	<dl
DB July 27 5-11m	7.2	9.3	2.6	0.3	<dl	<dl
DB July 27 12 m	7.3	10.4	1.4	0.3	<dl	<dl
DB July 27 14 m	5.5	10.9	0.8	0.4	<dl	<dl
DB July 27 16 m	5.6	11.1	0.2	0.4	<dl	<dl
DB July 27 18 m	5.8	11.9	0.0	0.4	<dl	<dl
DB July 27 20 m	5.9	12.2	0.0	0.4	<dl	<dl
DB Aug 10 0-3 m	7.6	7.4	7.8	5.5	<dl	<dl
DB Aug 10 4-11 m	5.4	9.3	2.5	5.0	<dl	<dl
DB Aug 10 12 m	7.8	11.0	0.2	4.5	<dl	0.05
DB Aug 10 14 m	8.4	11.4	0.1	4.3	<dl	<dl
DB Aug 10 16 m	7.7	11.1	0.1	4.2	<dl	<dl
DB Aug 10 18 m	7.7	12.0	0.1	4.1	<dl	0.03

Sample ID	DOC (mgC/L)	DIC (mgC/L)	δ13C-DIC	TDN (mg/L)	NO_2^- (mg/L)	NH_4^+ (mg/L)
DB Aug 10 20 m	8.2	13.0	0.1	3.9	<dl	0.04
DB Sep 1 0-5 m	5.3	8.0	7.5	6.2	<dl	0.29
DB Sep 1 6-13 m	6.1	10.3	1.1	4.8	<dl	<dl
DB Sep 1 14 m	6.9	12.3	0.1	6.7	<dl	0.07
DB Sep 1 16 m	7.1	12.4	0.2	4.3	<dl	0.11
DB Sep 1 18m	8.8	13.2	0.1	3.9	0.18	0.21
DB Sep 1 20m	9.3	14.0	0.1	3.7	<dl	0.28
DB Sep 14 0-6 m		8.6	7.4	6.1	<dl	<dl
DB Sep 14 7-11 m		10.6	1.4	4.7	<dl	<dl
DB Sep 14 12 m		12.0	0.2	4.2	<dl	<dl
DB Sep 14 14 m			0.2	4.0	<dl	<dl
DB Sep 14 16 m		13.7	0.1	5.6	<dl	0.18
DB Sep 14 18 m			0.2	4.0	<dl	0.25
DB Sep 14 20 m		14.1	0.2	4.1	<dl	0.08
DB Sep 28 0-8m		19.1	7.9	6.4		
DB Sep 28 9-12 m		12.9	0.6	4.5		
DB Sep 28 13m		8.4	0.2	4.2		
DB Sep 28 15 m		7.4	0.2	3.7		
DB Sep 28 17 m		7.1	0.2	3.3		